Title

Metabolic Cross-feeding Supports Growth of Candida albicans and Enterococcus faecalis in the Gut Microbiome

Author

Gause, Haley Elizabeth

Publication Date

2024

Peer reviewed|Thesis/dissertation

Metabolic Cross-Feeding Supports Growth of Candida albicans and Enterococcus faecalis in the Gut Microbiome

by

Haley Gause

DISSERTATION

Submitted in partial satisfaction of the requirements for degree of

DOCTOR OF PHILOSOPHY

in

Biochemistry and Molecular Biology

in the

GRADUATE DIVISION

of the

UNIVERSITY OF CALIFORNIA, SAN FRANCISCO

Approved:

DocuSigned by:
Carol Gross
F2413DA7F84F46A...
Carol Gross
Chair

DocuSigned by:
Alexander Johnson
D2BB5A36D2745B...
Alexander Johnson

DocuSigned by:
Susan Lynch
1A38FCA893D34C5...
Susan Lynch

Committee Members

Acknowledgements

Although graduate school often left me feeling very lonely and isolated within the never-ending to-do lists of experiments, it was also one of the first times of my life that I felt surrounded by a community in which I belonged. The work presented in this dissertation is the culmination of support I have received from many mentors, friends, colleagues and family, and I am immensely grateful for the impact each of them has had on my journey.

I would first like to thank my thesis advisor, Sandy Johnson. From the first day of my rotation, Sandy allowed me the intellectual freedom to pursue what I found interesting. This freedom allowed me to grow as a scientist and experience the inevitable failures that comes with scientific research. Sandy's steady encouragement gave me the confidence to keep moving forward, even when the path was unclear. I am deeply grateful for his mentorship and for teaching me the importance of good controls, to always re-focus on the question I am trying to answer, and how to think critically about science and data. In addition, my thesis committee, Carol Gross and Susan Lynch, experts in their respective fields of bacterial transcription and microbiome research, provided crucial interdisciplinary guidance. I'm grateful for their insights and enthusiasm.

While I have grown immensely as a scientist throughout graduate school, the scientific mentors I had before matriculating played a foundational role in shaping my journey. Dr. Jesse Dillon my academic advisor at CSULB, is the reason I became a scientific researcher. If not for his insistence semester after semester to join a research lab, I'm unsure where my path would have led. My first PI, Dr. Douglas Pace, provided me with invaluable experience from day one in his lab. It wasn't until I left CSULB that I realized how rare it is to join a lab and, within a week, be in the TC hood being trained to handle cells integral to the

entire lab's research. Dr. Pace placed significant responsibilities in my hands early on, and this hands-on experience boosted my confidence as an early-career scientist. I will be forever grateful for his trust, guidance, and support.

As part of the SRTP Program at UCSF, I had the opportunity to work in the lab of Shaeri Mukherjee. Shaeri's infectious enthusiasm for science, coupled with her encouragement during both the SRTP program and my subsequent time as a technician in her lab, played a big role in my decision to stay at UCSF for graduate school. I am thankful for her mentorship and support. Lastly, working under Rajita Pappu and Ena Ladi at Genentech as a summer intern was pivotal in redefining my vision of possible careers as a scientist. As my first introduction to industry, Ena and Rajita taught me invaluable lessons about how science is conducted outside the academic setting.

While I have learned a great deal directly from Sandy during my time in the Johnson Lab, I would argue that it is my fellow lab members who have taught me the most. Matt Lohse is an incredible experimentalist, and I consider myself fortunate to have learned how to troubleshoot and design experiments by working alongside him. Naomi Ziv taught me the importance of honesty and resilience in science—failure is just part of the job, even for the best scientists. I count myself lucky for getting to work alongside Kyle Fowler, for his experience and guidance in my early years in the lab played a huge role in thinking about my project and getting my work off the ground. Chien-der Lee is a powerhouse scientist; I am in awe of his ability to produce a tremendous amount of high-quality work. Megan Garber is always full of ideas and a great source of encouragement, and I am thankful for our thought-provoking discussions that sparked inspiration during the more challenging moments in the lab. Working alongside Francesca Del Frate is something I will cherish for the rest of my life.

The laughter, camaraderie, and stories we shared while working side-by-side in bay 3 were a constant source of motivation during the toughest periods, especially throughout the COVID-19 pandemic. Her support, both as a friend and a lab mate, is something I cannot fully put into words, but I am forever grateful for it. Jenny Zhang has been a constant sounding board and a trusted peer as we navigated bacterial-Candida interactions. Her calming presence, camaraderie, and thoughtful advice were crucial during our time together in the lab. I would also like to thank all of the past Johnson Lab members whose protocols and published papers made lab work a little less painful. Lastly, I would like to express my deepest gratitude to Ananda Mendoza, the true backbone of the Johnson Lab. None of the work presented in this thesis would have been possible without the thousands of plates and liters of media meticulously prepared by Ananda throughout my time in the lab. The Johnson Lab has been an incredible place for me to grow as a scientist, and I will always look back on my time in N374 with fondness.

While I am thankful for the scientific growth I experienced at UCSF, it pales in comparison to the growth I experienced as a person and that is all thanks to the incredible people and friends I have met along the way. It is rare for me to find people that I connect with on so many levels, but there must be something in the water at UCSF because I have found friends for life. Ady Steinbach was my first UCSF friend, and I am thankful she has always been there for me through this process. Katie Augspurger is a constant source of encouragement and inspiration. In a field of scientists, I never expected to find so many talented artists, sewists, and crafters. Being friends with Ady, Francesca and Katie inspires me to create and push myself as an artist, and I cannot put into words how thankful I am to have them serve on my committee of life.

I was lucky enough to live with Lili Kim and Natasha Puri throughout the pandemic. Their friendship was a great source of morale and laughter during an unsure time, and I will forever cherish my time at 330 Texas St. I would also like to thank a number of friends I've met through UCSF who have encouraged me and seen and accepted me for who I am: Luke Strauskulage, Henry Ng, Dana Kennedy, Elizabeth Bond, Varun Bhadkamkar, Nancy Chukwumezie and Cat Rodgers. Thank you for your friendship.

I would also like to thank Patricia Lee and Akshaya Uttamadoss for their friendship and support while I was in the trenches of graduate school. Our trips, conversations and dinners reminded me there is life outside of the lab and I respect and look up to both of them. Chelsea Powell is one of my dearest friends. From the first time we met during freshman orientation at CSULB, she has made me laugh, challenged me, and given me unwavering support. I am the woman I am today because of having Chelsea in my life. I have cherished our 10+ years of friendship and look forward to being friends for the rest of our lives.

No acknowledgement would be complete without thanking my family. My parents, Brock and Lonni, have always done everything they could to provide me with the opportunities and experiences to create and explore my passions and have always encouraged me to pursue my dreams. My dad is a dreamer and inventor, always asking the hows and whys of life. My mom is the hardest working person I know and her kindness and tenacity has always been an inspiration to me. Many of the skills that have allowed me to succeed in graduate school can be directly linked back to my Mom and Dad; they did an amazing job of fostering an insatiable sense of curiosity and creativity that are essential in a scientist. My sister Hannah is my biggest cheerleader and was always willing to go to bat for me. I appreciate her endless support. My dear niece Emerson, you are only two as I am

writing this, but you are already so smart. I am excited to see you grow and learn and will always be here to encourage you.

Lastly, thank you to my partner, Nica. You came into my life after a series of events no one could have predicted, so it must have been fate. Whereas science teaches one to lean into logic and reason, you have taught me the power of feeling my emotions. I have been lucky to finish graduate school with you by my side and look forward to our future together. I love you.

"Microbes are the invisible makers and shapers of the planet.

We live in a microbial world, where we are the newcomers."

Ed Yong

I Contain Multitudes: The Microbes Within Us and a Grander View of Life

Metabolic Cross-feeding Supports Growth of *Candida albicans* and *Enterococcus faecalis* in the Gut Microbiome

Haley Gause

Abstract

The adult gut microbiome is a diverse community of thousands of microorganisms spanning all three kingdoms of life. In contrast, the infant gut microbiome is relatively simple, offering a powerful, biologically relevant system to study foundational microbial community interactions. The fungal species *Candida albicans* and the bacterium *Enterococcus faecalis* are both common members of the infant gut microbiome, with co-occurrence of these two species widely reported across various dysbiotic gut environments. While previous studies suggest that *C. albicans* and *E. faecalis* interact in the gut, the mechanisms behind these interactions remain unclear. To more deeply probe the interaction between *C. albicans* and *E. faecalis* in the gut, we used dual RNA-sequencing to profile the transcriptional responses of both organisms during co-culture and compared them to individual growth under two conditions: (1) an *in vitro* condition designed to mimic certain aspects of the gut environment and (2) the germ-free mouse gut. Gene expression analysis of revealed that both species strongly upregulate citrate-related genes in each other's presence: *C. albicans* upregulates *CIT1* (citrate synthase) which produces citrate, while *E. faecalis* upregulates the entire *cit* operon, responsible for citrate metabolism. In *in vitro* co-cultures, we show that citrate is produced and secreted from *C. albicans* and consumed by *E. faecalis*, revealing a cross-feeding interaction. We further show that this citrate cross-feeding supports increased growth of *E. faecalis*, which depends on both *C. albicans*' expression of *CIT1* and *E. faecalis*' expression of the *cit* operon. Formate, a Short Chain Fatty Acid (SCFA) known to be toxic to

fungi, is a byproduct of citrate metabolism in *E. faecalis*. Indeed, we observed higher formate secretion from *E. faecalis* strains capable of metabolizing citrate. Our RNA profiling revealed that *C. albicans* strongly upregulates three formate dehydrogenases (FDHs) when co-cultured with *E. faecalis*. These FDHs detoxify formate and we show that their expression provides *C. albicans* with a growth advantage in the presence of formate. These findings reveal a metabolically driven interaction between *C. albicans* and *E. faecalis* in the gut, where cross-feeding of citrate and detoxification of formate facilitates the growth of both species when they are cultured together. Using a simplified fungal-bacterial co-culture system, our studies begin to reveal the mechanistic complexities of metabolic sharing between a eukaryote and a bacterium.

Table of Contents

List of Figures

Chapter 3

List of Tables

Chapter 2

Chapter 1

Introduction

The adult human gut microbiome is a complex community of microorganisms; the interactions among them shape large ecological and metabolic networks (Layeghifard et al., 2017; Shetty et al., 2022; Wang et al., 2024). This microbial community also interacts with the host to support numerous important aspects of human health, including maintenance of the gut epithelial layer and priming of the immune system (Lynch & Pedersen, 2016; Turroni et al., 2020). In addition, a diverse gut microbiome protects against perturbations to community homeostasis and the expansion of opportunistic microbial species (Chandra et al., 2021). Blooms of these pathobiont species are increasingly associated with many gastrointestinal, neurological, and immune disease states (Chandra et al., 2021; Manor et al., 2020).

While the gut microbiome is primarily comprised of bacterial species, it also includes a diverse array of other microorganisms, including viruses, archaea, and microeukaryotic species, including fungi (Gilbert et al., 2018). Fungi represent only a small fraction of the microbial population in a healthy gut microbiome. Multiple studies have reported fungal loads of healthy humans around 10^1–10^3 CFU per gram of feces compared to bacterial levels, which reach 10^{11}–10^{12} CFU per gram (Raimondi et al., 2019; Schulze & Sonnenborn, 2009). However, fungi are almost 100 times larger than bacteria by biomass, and their presence has been shown to significantly modulate the bacterial proteome within the gut micrbuobiome (Pettersen et al., 2022; Underhill & Iliev, 2014). This suggests that, despite their small numbers, fungi can exert a considerable influence in this environment, impacting bacterial activity and function.

One of the most common fungal colonizers of the gut microbiome is *Candida albicans*. This yeast species has been estimated to colonize between 75-95% of the adult human

population (Delavy et al., 2022, 2023; Nash et al., 2017). In addition, *C. albicans* is one of the first colonizers of the neonate gut microbiome and is estimated to colonize up to 96% of all infant guts (Schulze & Sonnenborn, 2009). *C. albicans*, like most fungal colonizers, is present in low numbers in a healthy gut microbiome. However, dysbiosis in the gut can lead to blooms of resident *C. albicans* as high as 10^5-10^7 CFU per gram of feces(Zhai et al., 2020). These fungal blooms have been observed to precede the onset of intestinal inflammation, epithelial barrier dysfunction, and translocation of *C. albicans* from the gut to bloodstream where it can cause systemic infection with mortality rates as high as 40% (Mazi et al., 2022; Sprague et al., 2022; Zhai et al., 2020)

In multiple studies of mouse models and human patients, blooms of *C. albicans* in dysbiotic gut microbiomes were associated with increases in the colonization of the bacterium *Enterococcus faecalis* (Mason et al., 2012; Seelbinder et al., 2023; Zhai et al., 2020). As with *C. albicans*, this firmicute is also found at low concentrations in the healthy gut but can become a dominant species in periods of dysbiosis (Lebreton et al., 2014; Repoila et al., 2022). Additionally, *E. faecalis* also can translocate across comprised gut barriers to cause fatal bloodstream infections (Archambaud et al., 2019; Ubeda et al., 2010). In addition, *Candida* and *E. faecalis* are among the most common colonizers of the pre-term infant gut microbiome. The gut microbiome of hospitalized preterm infants is exceptionally minimal and dysbiotic during the initial months of life (Thänert et al., 2024). This is attributed to several factors, including low maternal microbial colonization and the frequent use of antibiotics and antifungals in these infants (Levene et al., 2024; Thänert et al., 2024). In a recent metagenomic survey of pre-term infant gut microbiomes, *Candida* and *E. faecalis* were the primary components of some individuals (West et al., 2021). The correlation and

behavior of *C. albicans* and *E. faecalis* during gut dysbiosis suggests a complex interaction that may significantly impact host health.

Previous studies have begun to document some interactions between *E. faecalis* and *C. albicans*: *E. faecalis* has been shown to reduce hyphal formation in *C. albicans* and C. elegans colonized with both *C. albicans* and *E. faecalis* lead to a decrease in invasive growth typically observed when worms were colonized with either species alone(Cruz et al., 2013; Graham et al., 2017).

In this study, we describe the changes in gene expression when *C. albicans* and *E. faecalis* are cultured together compared to separate growth. Following up some on observed changes, we demonstrate a shared metabolic cycle in which *C. albicans* produces citrate, which is metabolized by *E. faecalis*, generating formate as a byproduct. This formate, in turn, induces the expression of formate-detoxifying enzymes in *C. albicans*. We propose that this type of metabolic cycle exemplifies the pairwise metabolic interactions between microbial species and in the gut.

References

Archambaud, C., Derré-Bobillot, A., Lapaque, N., Rigottier-Gois, L., & Serror, P. (2019). Intestinal translocation of enterococci requires a threshold level of enterococcal overgrowth in the lumen. *Scientific Reports*, *9*(1), 8926. https://doi.org/10.1038/s41598-019-45441-3

Chandra, H., Sharma, K. K., Tuovinen, O. H., Sun, X., & Shukla, P. (2021). Pathobionts: mechanisms of survival, expansion, and interaction with host with a focus on Clostridioides difficile. *Gut Microbes*, *13*(1), 1979882. https://doi.org/10.1080/19490976.2021.1979882

Cruz, M. R., Graham, C. E., Gagliano, B. C., Lorenz, M. C., & Garsin, D. A. (2013). Enterococcus faecalis Inhibits Hyphal Morphogenesis and Virulence of Candida albicans. *Infection and Immunity*, *81*(1), 189–200. https://doi.org/10.1128/iai.00914-12

Delavy, M., Burdet, C., Sertour, N., Devente, S., Docquier, J.-D., Grall, N., Volant, S., Ghozlane, A., Duval, X., Mentré, F., d'Enfert, C., Bougnoux, M.-E., & Group, P. S. (2022). A Clinical Study Provides the First Direct Evidence That Interindividual Variations in Fecal β-Lactamase Activity Affect the Gut Mycobiota Dynamics in Response to β-Lactam Antibiotics. *MBio*, *13*(6), e02880-22. https://doi.org/10.1128/mbio.02880-22

Delavy, M., Sertour, N., Patin, E., Chatelier, E. L., Cole, N., Dubois, F., Xie, Z., Saint-André, V., Manichanh, C., Walker, A. W., Quintana-Murci, L., Duffy, D., d'Enfert, C., Bougnoux, M.-E., & Consortium, M. I. (2023). Unveiling Candida albicans intestinal carriage in healthy

volunteers: the role of micro- and mycobiota, diet, host genetics and immune response. *Gut Microbes*, *15*(2), 2287618. https://doi.org/10.1080/19490976.2023.2287618

Gilbert, J. A., Blaser, M. J., Caporaso, J. G., Jansson, J. K., Lynch, S. V., & Knight, R. (2018). Current understanding of the human microbiome. *Nature Medicine*, *24*(4), 392–400. https://doi.org/10.1038/nm.4517

Graham, C. E., Cruz, M. R., Garsin, D. A., & Lorenz, M. C. (2017). Enterococcus faecalis bacteriocin EntV inhibits hyphal morphogenesis, biofilm formation, and virulence of Candida albicans. *Proceedings of the National Academy of Sciences*, *114*(17), 4507–4512. https://doi.org/10.1073/pnas.1620432114

Layeghifard, M., Hwang, D. M., & Guttman, D. S. (2017). Disentangling Interactions in the Microbiome: A Network Perspective. *Trends in Microbiology*, *25*(3). https://doi.org/10.1016/j.tim.2016.11.008

Lebreton, F., Willems, R. J. L., & Gilmore, M. S. (2014). Enterococcus Diversity, Origins in Nature, and Gut Colonization Abstract Introduction. In M. S. Gilmore, D. B. Clewell, Y. Ike, & N. Shankar (Eds.), *Enterococci From Commensals to Leading Causes of Drug Resistant Infection*. Boston: Massachusetts Eye and Ear Infirmary.

Levene, I., Harrison, S., Alderdice, F., & Quigley, M. A. (2024). Breastfeeding trajectories for preterm infants over the first 6 months of life in England 2010–2020: surveys using large representative birth samples. *BMJ Paediatrics Open*, *8*(1), e002912. https://doi.org/10.1136/bmjpo-2024-002912

Lynch, S. V., & Pedersen, O. (2016). The Human Intestinal Microbiome in Health and Disease. *The New England Journal of Medicine*, *375*(24), 2369–2379. https://doi.org/10.1056/nejmra1600266

Manor, O., Dai, C. L., Kornilov, S. A., Smith, B., Price, N. D., Lovejoy, J. C., Gibbons, S. M., & Magis, A. T. (2020). Health and disease markers correlate with gut microbiome composition across thousands of people. *Nature Communications*, *11*(1), 5206. https://doi.org/10.1038/s41467-020-18871-1

Mason, K. L., Downward, J. R. E., Mason, K. D., Falkowski, N. R., Eaton, K. A., Kao, J. Y., Young, V. B., & Huffnagle, G. B. (2012). Candida albicans and Bacterial Microbiota Interactions in the Cecum during Recolonization following Broad-Spectrum Antibiotic Therapy. *Infection and Immunity*, *80*(10), 3371–3380. https://doi.org/10.1128/iai.00449-12

Mazi, P. B., Olsen, M. A., Stwalley, D., Rauseo, A. M., Ayres, C., Powderly, W. G., & Spec, A. (2022). Attributable Mortality of Candida Bloodstream Infections in the Modern Era: A Propensity Score Analysis. *Clinical Infectious Diseases*, *75*(6), 1031–1036. https://doi.org/10.1093/cid/ciac004

Nash, A. K., Auchtung, T. A., Wong, M. C., Smith, D. P., Gesell, J. R., Ross, M. C., Stewart, C. J., Metcalf, G. A., Muzny, D. M., Gibbs, R. A., Ajami, N. J., & Petrosino, J. F. (2017). The gut mycobiome of the Human Microbiome Project healthy cohort. *Microbiome*, *5*(1), 153. https://doi.org/10.1186/s40168-017-0373-4

Pettersen, V. K., Dufour, A., & Arrieta, M.-C. (2022). Metaproteomic profiling of fungal gut colonization in gnotobiotic mice. *Animal Microbiome*, *4*(1), 14. https://doi.org/10.1186/s42523-022-00163-2

Raimondi, S., Amaretti, A., Gozzoli, C., Simone, M., Righini, L., Candeliere, F., Brun, P., Ardizzoni, A., Colombari, B., Paulone, S., Castagliuolo, I., Cavalieri, D., Blasi, E., Rossi, M., & Peppoloni, S. (2019). Longitudinal Survey of Fungi in the Human Gut: ITS Profiling, Phenotyping, and Colonization. *Frontiers in Microbiology*, *10*, 1575. https://doi.org/10.3389/fmicb.2019.01575

Repoila, F., Bohec, F. L., Guérin, C., Lacoux, C., Tiwari, S., Jaiswal, A. K., Santana, M. P., Kennedy, S. P., Quinquis, B., Rainteau, D., Juillard, V., Furlan, S., Bouloc, P., Nicolas, P., Miyoshi, A., Azevedo, V., & Serror, P. (2022). Adaptation of the gut pathobiont Enterococcus faecalis to deoxycholate and taurocholate bile acids. *Scientific Reports*, *12*(1), 8485. https://doi.org/10.1038/s41598-022-12552-3

Schulze, J., & Sonnenborn, U. (2009). Yeasts in the Gut. *Deutsches Ärzteblatt International*, *106*(51–52), 837–842. https://doi.org/10.3238/arztebl.2009.0837

Seelbinder, B., Lohinai, Z., Vazquez-Uribe, R., Brunke, S., Chen, X., Mirhakkak, M., Lopez-Escalera, S., Dome, B., Megyesfalvi, Z., Berta, J., Galffy, G., Dulka, E., Wellejus, A., Weiss, G. J., Bauer, M., Hube, B., Sommer, M. O. A., & Panagiotou, G. (2023). Candida expansion in the gut of lung cancer patients associates with an ecological signature that supports growth under dysbiotic conditions. *Nature Communications*, *14*(1), 2673. https://doi.org/10.1038/s41467-023-38058-8

Shetty, S. A., Kuipers, B., Atashgahi, S., Aalvink, S., Smidt, H., & Vos, W. M. de. (2022). Inter-species Metabolic Interactions in an In-vitro Minimal Human Gut Microbiome of Core Bacteria. *Npj Biofilms and Microbiomes*, *8*(1), 21. https://doi.org/10.1038/s41522-022-00275-2

Sprague, J. L., Kasper, L., & Hube, B. (2022). From intestinal colonization to systemic infections: Candida albicans translocation and dissemination. *Gut Microbes*, *14*(1), 2154548. https://doi.org/10.1080/19490976.2022.2154548

Thänert, R., Schwartz, D. J., Keen, E. C., Hall-Moore, C., Wang, B., Shaikh, N., Ning, J., Rouggly-Nickless, L. C., Thänert, A., Ferreiro, A., Fishbein, S. R. S., Sullivan, J. E., Radmacher, P., Escobedo, M., Warner, B. B., Tarr, P. I., & Dantas, G. (2024). Clinical sequelae of gut microbiome development and disruption in hospitalized preterm infants. *Cell Host & Microbe*, *32*(10), 1822-1837.e5. https://doi.org/10.1016/j.chom.2024.07.027

Turroni, F., Milani, C., Duranti, S., Lugli, G. A., Bernasconi, S., Margolles, A., Pierro, F. D., Sinderen, D. van, & Ventura, M. (2020). The infant gut microbiome as a microbial organ influencing host well-being. *Italian Journal of Pediatrics*, *46*(1), 16. https://doi.org/10.1186/s13052-020-0781-0

Ubeda, C., Taur, Y., Jenq, R. R., Equinda, M. J., Son, T., Samstein, M., Viale, A., Socci, N. D., Brink, M. R. M. van den, Kamboj, M., & Pamer, E. G. (2010). Vancomycin-resistant Enterococcus domination of intestinal microbiota is enabled by antibiotic treatment in mice and precedes bloodstream invasion in humans. *Journal of Clinical Investigation*, *120*(12), 4332–4341. https://doi.org/10.1172/jci43918

Underhill, D. M., & Iliev, I. D. (2014). The mycobiota: interactions between commensal fungi and the host immune system. *Nature Reviews Immunology*, *14*(6), 405–416. https://doi.org/10.1038/nri3684

Wang, S., Mu, L., Yu, C., He, Y., Hu, X., Jiao, Y., Xu, Z., You, S., Liu, S.-L., & Bao, H. (2024). Microbial collaborations and conflicts: unraveling interactions in the gut ecosystem. *Gut Microbes*, *16*(1), 2296603. https://doi.org/10.1080/19490976.2023.2296603

West, P. T., Peters, S. L., Olm, M. R., Yu, F. B., Gause, H., Lou, Y. C., Firek, B. A., Baker, R., Johnson, A. D., Morowitz, M. J., Hettich, R. L., & Banfield, J. F. (2021). Genetic and behavioral adaptation of Candida parapsilosis to the microbiome of hospitalized infants revealed by in situ genomics, transcriptomics, and proteomics. *Microbiome*, *9*(1), 142. https://doi.org/10.1186/s40168-021-01085-y

Zhai, B., Ola, M., Rolling, T., Tosini, N. L., Joshowitz, S., Littmann, E. R., Amoretti, L. A., Fontana, E., Wright, R. J., Miranda, E., Veelken, C. A., Morjaria, S. M., Peled, J. U., Brink, M. R. M. van den, Babady, N. E., Butler, G., Taur, Y., & Hohl, T. M. (2020). High-resolution mycobiota analysis reveals dynamic intestinal translocation preceding invasive candidiasis. *Nature Medicine*, *26*(1), 59–64. https://doi.org/10.1038/s41591-019-0709-7

Chapter 2

Methods

Strains, Media, and Growth Conditions

Candida albicans and *Enterococcus faecalis* strains and media in this study are detailed in Tables 2.1 & 2.2. *C. albicans* strain SC5314 was used as the wild-type strain for all experiments and used to derive all mutant strains. *E. faecalis* strain OG1RF was the wild-type and parental strain for all experiments and mutant generation. Strains were maintained as glycerol stocks and stored at -80C. Unless otherwise stated, *in vitro* experiments were performed in an Anaerobic Chamber (Coy Lab) set at the following parameters: 0.2% O_2, 5% CO_2, ambient air temperature (hereby referred to as "hypoxic chamber".) All media and consumable reagents (e.g. plates, serological pipettes, pipette tips) were moved into the chamber at least 1 day before the start of experiments to de-oxygenate. Strains were struck in ambient air onto Brain Heart Infusion (BHI) agar plates, after which the plates were ported into the chamber and placed in a 37^{o}C incubator. Experimental liquid cultures were grown in 24 deep-well plates at 37^{o}C with agitation (800 RPM).

C. albicans Mutant Generation

Plasmid and primers used in strain construction are detailed in Tables 2.3 and 2.4. Gene deletion mutants in *C. albicans* were constructed using a CRISPR-Cas9 method detailed in (Lee & Johnson, 2024)modified from (Nguyen et al., 2017). Instead of 80bp of homology, only 60bp of homology directly flanking the start and stop codons were used to construct the repair template.

E. faecalis Mutant Generation

Primers and plasmids used in strain construction are detailed in Tables 2.3 and 2.4. Gene deletion mutants in *E. faecalis* were constructed using the CRISPR-Cas12 method outlined in (Chua & Collins, 2022), with some modifications. Briefly, pJC005.em was restriction digested or amplified. Three inserts (pUCsRNAP-gRNA, 650 bp upstream homology to the gene, and 650bp downstream homology) were amplified via PCR, inserted into the linearized backbone using Gibson Assembly (NEB), and transformed into NEB DH5α cells. After confirming via sequencing, the constructed plasmid was transformed into *E. faecalis* OG1RF following the protocol outlined in (Fozo, 2020). Todd Hewitt Broth (THB) + 10ug/ml erythromycin agar plates were used for selection post-transformation. All subsequent steps used BHI media and agar plates with added 10ug/ml erythromycin and 250 ng/ml anhydrous tetracycline when needed.

Cell Growth for *in vitro* RNA-seq

Single colonies of *C. albicans* and *E. faecalis* (from BHI plates grown for one day at 37^{o}C in hypoxic chamber) were inoculated in 2ml BHI media (BD Difco) and grown overnight. In the morning, cultures were backdiluted to OD of 0.1 in 6ml BHI media and grown as above for 4 hours. *C. albicans* was backdiluted to an OD600 of 0.2 in BHI media, and *E. faecalis* cells were centrifuged and re-suspended in fresh BHI media at an OD600 of 2. Both *C. albicans* and *E. faecalis* in the experimental co- and mono-cultures were started at an OD of 0.2 in 2ml BHI media. Experimental cultures were grown at 37^{o}C for 4 hours, after which they were harvested by centrifugation (3500 RPM for 5 min) and pellets were flash frozen and stored at -80^{o}C.

Colonization of Germ-Free Mice Gastrointestinal Tract

C. albicans strains were grown overnight in Yeast Peptone Dextose (YPD) media (2% Bacto peptone, 2% dextrose, 1% yeast extract) at 30^{o}C and *E. faecalis* strains were grown overnight in BHI media at 37^{o}C. Cells were washed twice in sterile Phosphate Buffer Saline (PBS) and concentration was determined using a BD Accuri C6 flow cytometer. All mice work was performed in the UCSF Gnotobiotics Core Facility. Mice were kept in cages contained within a sterile isolator for the duration of the experiment. A minimum of 8 germ-free C57BL/6 mice of mixed sex were colonized via gavage with i) 3x10^{6} *C. albicans* cells, ii) 3x10^{6} *C. albicans* cells and 5x10^{8} *E. faecalis* cells, or iii) 5x10 ^{8} *E. faecalis* cells in 0.1ml PBS. At the end of 10 days, mice were euthanized, and the cecum contents were added to 5ml RNAlater stabilization solution (Invitrogen AM7020), and placed at 4^{o}C. After 1 day at 4^{o}C, cecum contents-RNAlater slurries were aliquoted, centrifuged and the RNAlater supernatant was removed. Cecum content pellets were stored in -80^{o}C until used for downstream processing.

Plating of Fecal Pellets to Determine Microbial Burden

Colonization of gnotobiotic mice was monitored by the collection and plating of fecal pellets at 3 and 10 days post gavage. The wet weight of a fecal pellet was recorded. Pellet was then homogenized in 500µL sterile PBS via vortexing. PBS-fecal slurry was serially diluted and plated on YPD + 250 µg/mL erythromycin (yeast-selection) or BHI + 50 ug/ml nystatin (bacteria-selection). Yeast plates were grown at 30^{o}C and bacteria plates were grown at 37^{o}C overnight. Colony forming units (CFUs) were enumerated and calculated relative to the starting weight of the pellet to determine CFU/g fecal pellet.

RNA Extraction from *in vitro* samples and Cecum Contents

RNA was extracted from cecal contents using a protocol based on (Turnbaugh et al., 2009) that was optimized to yield high purity and quantity RNA from gnotobiotic mice. Full protocol can be found in Supplementary Methods S1 and in the following reference: (Gause, 2022)

For *in vitro* samples, RNA was extracted using same protocol with few modifications: only 1 additional phenol-chloroform extraction was performed prior to isopropanol precipitation. For all RNA samples, concentration of total RNA was determined using a Nanodrop and RNA integrity was analyzed using Tapestation High-Sensitivity RNA kit (Agilent 5067-5579).

rRNA depletion and Library Preparation

rRNA was depleted from total RNA using filamentous-fungi riboPOOL, Pan-Bacteria riboPOOL, and Mus musculus riboPOOL (siTOOLs) using manufacturer's protocol with some modifications. For dual-species *in vitro* samples, bacteria and fungi riboPOOL probes were mixed at a 3:1 ratio. For dual-species cecum content samples, probes were mixed at a 8:1:1 bacteria:fungi:mouse ratio. For all single species samples, the probes for the specific species were used alone. 1.5 – 2 µg total RNA was used as input. Remaining RNA was concentrated using Zymo clean & concentrator-5. RNA concentration was determined using Qubit High-Sensitivity RNA kit and success of depletion was determined using Tapestation High-Sensitivity RNA kit (Agilent 5067-5579).

RNA-seq libraries were created using CORALL Total RNA-seq V1 kit (Lexogen 095) according to manufacturer protocol. 5 ng of rRNA-depleted RNA was used as input into

library generation. Concentration and average size of resulting DNA library determined using Tapestation High-Sensitivity DNA kit (Agilent 5067-5584). Libraries were pooled in equimolar amounts and sequenced at the Chan Zuckerberg Biohub on the Illumina NextSeq Platform with the following parameters: 100bp single-end read, minimum of 35 million reads per sample.

RNA-seq Analysis

RNA-seq reads were filtered for quality and trimmed of Illumina sequencing adapters and polyA tails using Fastp (0.20.1) (Chen et al., 2018). FastQC (0.11.9) was used to perform quality checks of data (Andrews, 2010). Reads were mapped using STAR (2.7.9a)(Dobin et al., 2013). *C. albicans* mono-cultures were mapped to the *C. albicans* SC5314 Assembly 22 (version A22-s07-m01-r105) chromosomes file from Candida Genome Database (CGD)(Skrzypek et al., n.d.), modified to contain only A allele chromosomes and novel transcripts found in (Tuch et al., 2010). *E. faecalis* mono-cultures were mapped to the *E. faecalis* OG1RF genome (ASM17257v2, assembly 46) from EnsembleBacteria (Harrison et al., 2023). Reads from co-culture samples were mapped simultaneously onto a concatenated *C. albicans-E. faecalis* genome. After alignment, resulting BAM files were filtered using Samtools (1.14) to discard any reads less than 30bp long (Danecek et al., 2021). These reads, despite being a small proportion of the total mapped reads (<3%) were found to erroneously map and create false positives in downstream results, especially in otherwise lowly expressed genes. Read counts for each species were then extracted using Subread FeatureCounts (2.0.1) using the appropriate genome version specific GFF file(Liao et al., 2014). Count normalization and differential expression analysis was performed using

DESeq2 (1.40.2) (Love et al., 2014). Mouse and *in vitro* samples were loaded and processed as separate DESeq objects. Counts tables were filtered after generating DESeq objects to only contain genes with more than 10 raw counts in at least 3 samples.

Gene Expression Measurements via RT-qPCR

To measure the gene expression of various genes in either *C. albicans* or *E. faecalis*, mono- or co-cultures were grown as outlined in the *in vitro* RNA-seq section of the methods above. Overnight and outgrowth cultures were grown in BHI media (Alpha Biosciences) with added 0.2% sodium citrate. Media used in experimental cultures is detailed in Table 2.2 with or without added 0.2% sodium citrate. Total RNA was extracted from frozen cell pellets following the RNA-extraction protocol detailed above with modifications: 1) only 1 phenol-chloroform extraction was performed prior to isopropanol precipitation, 2) no column clean-up was used (post-precipitation RNA was used directly in DNase treatment) and 3) no lithium chloride precipitation was used. RNA concentration was measured using a nanodrop and RNA integrity was measured using Tapestation High Sensitivity RNA kit. cDNA was generated from 450 ng of total RNA using LunaScript® RT SuperMix Kit (New England Biolabs E3010). RT-qPCR was performed with iTaq Universal SYBR Green Supermix (Biorad 1725124) in 5 µL reaction volumes with 1µL of cDNA (diluted 1:4 before use). Primers listed in Table 2.5 were used at a final concentration of 0.3µM. A minimum of 3 technical replicates was measured per sample-primer pair.

The *in vitro* RNA-seq expression data generated in this study was used for *C. albicans* and *E. faecalis* housekeeping gene selection. Two housekeeping genes were selected per species based on the following criteria: 1) Log_2 Fold Change in expression between co-

culture and mono-culture between -0.25 and 0.25, 2) annotated role in core, essential processes (e.g. DNA replication, cell cycle machinery, RNA polymerase subunits), 3) one lowly expressed and one highly expressed gene. Based on this criteria, *C. albicans* housekeeping genes used in this study were *ORF19.6843* and *IRR1*, and *E. faecalis* housekeeping genes used were *dnaA* and *rpoB*. Results were analyzed using the ΔΔCt method, with Ct values for each sample normalized to the average Ct value of the two housekeeping genes.

Citrate Measurements

Supernatants of samples grown for qPCR assays were filter-sterilized with a 0.2μM Polyethersulfone (PES) filters and flash-frozen using liquid nitrogen until use in downstream assays. Citrate concentrations were measured using Citric Acid Kit (Megazyme K-CITR) following manufacturer's microplate assay procedure using ½ volume reactions. Absorbance was measured using a Tecan Spark 10M.

For high-sensitivity citrate measurement, citrate levels were quantified at the UCSF Quantitative Metabolite Analysis Center using liquid chromatography-mass spectrometry (LC-MS) with validated internal standards and citrate-specific calibration curves for quantification. Quality control and data processing were managed using the center's custom software.

***E. faecalis* growth curves with or without citrate in hypoxic conditions**

Single colonies of *E. faecalis* strains (from BHI plates grown at 37^{o}C for one day in hypoxic chamber) were used to inoculate 2ml of BHI media (Alpha Biosciences) with added

0.2% sodium citrate. Cultures were washed twice and resuspended in PBS, and back-diluted into 100ul of various BHI medias (detailed in Table 2.2) with or without added 0.2% sodium citrate at a final OD600 of 0.01 in a flat-bottom, clear 96-well plate. 100µL of each media was included on the plate as a blank control. OD600 of each well was measured every 15 min with shaking between each time point using a Tecan Infinite Nano M Plus in the hypoxic chamber. At each time point, the absorbance value of each well was corrected by subtracting the absorbance value of the corresponding blank media well.

E. faecalis Growth Assays in the presence of *C. albicans* in hypoxic conditions

Single colonies of *E. faecalis* or *C. albicans* strains (from BHI agar plates grown at 37^{o}C for one day in hypoxic chamber) were used to inoculate 2ml of BHI media (Alpha Biosciences) with added 0.2% sodium citrate. Cultures were washed twice and resuspended in PBS. Experimental cultures were inoculated into 2ml various BHI medias (detailed in Table 2.2) with or without added 0.2% sodium citrate at a starting OD600 of 0.1 for *C. albicans* and 0.01 for *E. faecalis*. Cultures were grown at 37^{o}C with agitation for 24 hours. Aliquots from 24 hour cultures were 10-fold serially diluted and 100uL of the 10^{6} dilution was plated on BHI + 50 ug/ml nystatin plates to select for *E. faecalis*. Colonies were enumerated and used to calculate CFU/ml of cultures.

Formate Measurements

Supernatants of cultures were filter-sterilized with a 0.2µM Polyethersulfone (PES) filters and flash-frozen using liquid nitrogen until use in downstream assays. Formate concentrations were measured using Formic Acid Assay Kit (Megazyme K-FORM) following

manufacturer's microplate assay procedure using ½ volume reactions. Absorbance (340nm) was measured using a Tecan Spark 10M.

C. albicans Growth Curve in Formate

Single colonies of *C. albicans* WT and single, double, and triple knockouts of formate dehydrogenase genes (see Table 2.1 for details) were inoculated into 300uL PBS and vortexed to resuspend. Cells in PBS were diluted to a final OD600 of 0.005 in 100 µl of various media (see Table 2.2 for details) with or without the addition of 3% sodium formate (equivalent to 2% formate) in a flat-bottomed 96-well plate. 100µL of each media was included on the plate as a blank control. OD600 of each well was measured every 15 min with shaking between each time point using a Tecan Spark 10M in aerobic conditions. At each time point, the absorbance value of each well was corrected by subtracting the absorbance value of the corresponding blank media well.

Supplementary Methods S1

RNA Extraction from Cecum Contents of Gnotobiotic Mice

This protocol was designed to extract RNA from the cecum contents of gnotobiotic mice colonized with relatively simple gut microbiomes. The cecum from these mice contain high amounts of undigested polysaccharides and polyphenols that can inhibit the extraction of high yield, pure RNA. By increasing the number of phenol/chloroform extractions and introducing a final precipitation using lithium chloride, we were able to extract large amounts of RNA

(> 10mg) with high purity ($A_{260/280}$ = > 2.0, $A_{260/230}$ = 2.0-2.3).

At the time of mouse euthanasia:

1. Drop ½ of cecum contents into 10 ml RNAlater. Leaves tubes at 4^{o}C for 1 day.
2. Pre-weigh 2ml microcentrifuge tubes. Add 1ml of RNAlater-cecum content slurry to each tube (~200mg contents) and centrifuge at 3500RPM for 5 min to pellet contents.
3. Weigh pellets. Store aliquots at -80^{o}C.

RNA extraction:

1. To 2ml RNase-free screw cap tube, add ~500µL ice-cold 0.5µM zirconia beads (4 per cecum aliquot – 1 per 100mg). Keep tubes on ice until use.
2. Place cecum content aliquots on ice to thaw.
3. Resuspend aliquot in the following per 100mg (4x – multiple all volumes by 4):
    a. 500µL Lysis Buffer (200 mM NaCl, 20mM EDTA)
    b. 210µL 20% SDS
    c. 500µL phenol:chloroform:isoamyl alcohol (PCI) (pH 4.5, 125:24:1)

4. Transfer resuspended cecum contents to screw-cap tube containing beads. Split total volume between 2 bead-beating tubes (each has ~1210uL)
5. Bead-beat 5min using Mini-beadbeater
6. Centrifuge at 10000xg for 5 minutes to separate phases
7. Transfer aqueous phase to new microcentrifuge tube. Add equal volumes phenol:chloroform:isoamyl alcohol (PCI) and vortex 20s. Spin @ 10000xg for 5 minutes.
8. Transfer aqueous phase to phase-lock tube. Add equal volume of PCI, shake well to mix and @ 10000xg for 3 minutes.
9. Add equal volume PCI to aqueous above the phase-lock layer, mix well by shaking and spin @ 10000xg for 3 minutes.
10. Repeat step 9 two more times (total of 6 Phenol chloroform extractions)

Isopropanol Precipitation

11. Decant aqueous phase to new RNase-free microcentrifuge tube. Add 1 volume RT isopropanol and place at -20C for 20 minutes.
12. Centrifuge at max speed for 25 min, 4C. You will see a disk of RNA form between two layers (don't know why it's a disk, why there are layers, why anything really)
13. Carefully remove ALL liquid from tube (above and below disk of nucleic acid). If you don't remove the liquid below the disk, the carbohydrates will begin to crash out and crystalize when doing the EtOH washes → less pure
14. Wash 2X with 750µl 75% ethanol. Invert to wash tube. Centrifuge max speed for 5 minutes, 4^{o}C.

15. Remove all ethanol from pellet (remove supernatant, quick spin, remove residual ethanol with aspirator). Air dry pellet for <5 min if a lot of residual ethanol remains.
16. Resuspend pellet in 50 µL 45°C nuclease-free water
    a. Make sure pellet is completely resuspended before moving forward! Place at 45°C for a few minutes to fully resuspend

NEB Monarch RNA Clean-up (500ug) (T2050)

1. Follow manufacturers protocol:
    a. Add 2X RNA Cleanup Buffer (100ul to 50ul sample)
    b. Add 1 vol 100% ethanol to sample (150ul)
    c. Invert/flick to mix
    d. Transfer to Spin-cartridge. Spin at 12000xg for 1min. Discard flow-through
    e. Add 700µL wash buffer I. Centrifuge and discard flow-through
    f. Wash 2X with 500µL wash buffer II. Centrifuge and discard flow-through.
    g. Centrifuge spin-cartridge ~ 12000xg for 1 min to dry membrane.
    h. Place dried membrane in clean Eppendorf tube.
    i. Add 50ul nuclease-free water to center of membrane. Let incubate at RT for 1 min. Centrifuge to collect flow-through.

Ambion TURBO DNA-free Kit (AM1907)

2. Follow manufacturers protocol:
    a. To 50µL sample, add and mix gently:
        i. 5 µL 10X buffer
        ii. 1 µl TURBO DNA
    b. Incubate at 37°C for 20-30 minutes

c. Resuspend DNAse Inactivation Reagent by vortexing. Add 6 µL inactivation reagent to samples and mix by flicking.
d. Incubate at RT for 5 minutes. Flick tube occasionally to resuspend inactivation reagent.
e. Centrifuge tube @ 10000xg for 1.5 minutes. Carefully transfer 50ul into new tube.

Lithium Chloride Precipitation

3. Add 25ul 7.5M Lithium chloride precipitation solution (final= 2.5M) and 1ul glycoblue co-precipitant Store at -20C overnight
4. Centrifuge at max speed for 25 min, 4C. You should see large, gelatinous pellet form at bottom of tube.
5. Wash 2X with 750µl ice-cold 75% ethanol. Vortex tubes ~30s to completely wash tube and pellet. Centrifuge max speed for 5 minutes, 4C.
6. Remove all ethanol from pellet (remove supernatant, quick spin, remove residual ethanol with aspirator). Air dry pellet for <5 min if a lot of residual ethanol remains.
7. Resuspend pellet in 30 µL 50°C nuclease-free water
    a. Make sure pellet is completely resuspended before moving forward!

Table 2.1: *C. albicans* and *E. faecalis* strains used in this study

C. albicans Strains				
Strain Name	Description/Informal Name	Genotype	Parent	Source
SC5314	WT	WT	—	
yHG140	*Δcit1*	*cit1Δ/cit1Δ*	SC5314	This study
yHG146	*Δfdh1*	*fdh1Δ/fdh1Δ*	SC5314	This study
yHG169	*Δorf19.1117*	*orf19.1117Δ/orf19.1117Δ*	SC5314	This study
yHG135	*Δorf19.1774*	*orf19.1774Δ/orf19.1774Δ*	SC5314	This study
yHG153	*Δfdh1/Δorf19.1774*	*fdh1Δ/fdh1Δ; orf19.1774Δ/orf19.1774Δ*	yHG146	This study
yHG154	*Δorf19.1774/Δfdh1*	*orf19.1774Δ/orf19.1774Δ; fdh1Δ/fdh1Δ*	yHG135	This study
yHG171	*FDHΔ3 isolate 1 (Δfdh1/Δorf19.1774/ Δorf19.1117)*	*fdh1Δ/fdh1Δ; orf19.1774Δ/orf19.1774Δ; orf19.1117Δ/ orf19.1117Δ*	yHG153	This study
yHG173	*FDHΔ3 isolate 2 (Δorf19.1774/Δfdh1 Δorf19.1117)*	*orf19.1774Δ/orf19.1774Δ; fdh1Δ/fdh1Δ; orf19.1117Δ/ orf19.1117Δ*	yHG154	This study
E. faecalis Strains				
Strain Name	Description/Informal Name	Genotype	Parent	Source
OG1RF	WT	WT	_	(Murray et al., 1993)
bHG35	Δ*citHO*	Δ*citH*;Δ*citO*	OG1RF	This study
bHG39	ΔpflAB	Δ*pflA*;Δ*pflB*	OG1RF	This study

Table 2.2: Media Used in this Study

*Lack of citrate is not denoted by manufacturer, but was empirically determined using Citrate Acid Kit (see methods)

Media Name	Source	Nutrient Description (from manufacturer)	Added Nutrients in this study	Assay Used In
BHI Difco	BD Difco™ 237500	0.2% dextrose	—	RNA-seq
BHI	Alpha Biosciences (B02-113-500)	0.2% dextrose, no citrate*	—	Growth assays, qPCR, citrate and formate measurements
BHI-glucose (BHI-g)	Alpha Biosciences (B02-114-500)	No added dextrose, no citrate*	—	Growth assays, qPCR, citrate and formate measurements

Table 2.3: Plasmids

Name	Description	Used in	Source
pADH34	SAT1-Knock Out dDNA Template	*C. albicans* mutant strain construction	(Hernday et al., 2010)
pADH143	Knock Out gRNA Template	*C. albicans* mutant strain construction	(Nguyen et al., 2017)
pp2280	P_{ENO1}-Cas9-T_{CYC1} construct	*C. albicans* mutant strain construction	
pJC005.em	(Empty Backbone) CRISPR-Cas12a genome editing of E. faecium	*E. faecalis* mutant strain plasmid construction	Gifted from James Collins (Chua & Collins, 2022) (Addgene # 182738)
pUCsRNAP	Swapping in small RNA promoter, 23-bp spacer sequence, & 19-bp repeats into pJC005 plasmids	*E. faecalis* mutant strain plasmid construction	Gifted from James Collins (Chua & Collins, 2022) (Addgene # 182746)
pHG3	pJC005.em backbone; insert: gRNA(citH)-citH upstream homology-citO downstream homology	*E. faecalis* mutant strain construction	This study
pHG7	pJC005.em backbone; insert: gRNA(pflB)-pflB upstream homology-pflA downstream homology	*E. faecalis* mutant strain construction	This study

Table 2.4: Primers Used in Strain Construction

Bolded bases in primer sequences denote the gRNA used in CRISPR strain construction

Primer Name	Primer Sequence	Used for
oHG85_PSNR52_F	catctaatcaactcccagat	*C. albicans* Mutant Generation – PSNR fragment 1
oHG86_PSNR52_R	caaattaaaaatagtttacgcaa	*C. albicans* Mutant Generation – PSNR fragment 1
oHG212_CIT1_gRNA_F	cttgcgtaaactatttttaatttg**aaacaattcaaaaaagaaca**gttttagagctagaaatagca	*C. albicans* Δ*cit1* Generation – PSNR fragment 2
oHG88_gRNA-scaffoldTerminator_R	taaaaaaactcgagaaaaaaagcac	*C. albicans* Δ*cit1* Generation – PSNR fragment 2
oHG210_CIT1_ downhomology_SAT1_R	atcattgaataataaataataataaataaaatctagtcaaacaggatacccgtcaaatcacgctctagaactagtggatc	*C. albicans* Δ*cit1* Generation – homology flanked repair template
oHG211_CIT1_uphomology_SAT1_F	tcttcttttccttttcccatcttttaagtttcttttagaatatagtatatttatcaaacactagtgaattcgcgctcgag	*C. albicans* Δ*cit1* Generation – homology flanked repair template
oHG208_CIT1_orfcheck_R	ctgtaaatcttagcagcaatgg	*C. albicans* Δ*cit1* Generation – ORF check
oHG209_CIT1_orfcheck_F	gggaaggttctgttttggac	*C. albicans* Δ*cit1* Generation – ORF check
oHG211_CIT1_ uphomology_SAT1_F	tcttcttttccttttcccatcttttaagtttcttttagaatatagtatatttatcaaacactagtgaattcgcgctcgag	*C. albicans* Δ*cit1* Generation – flank check
oHG226_CIT1_ downflankcheck_R	agagcaccaccaatagtttc	*C. albicans* Δ*cit1* Generation – flank check
oHG185_RNAP_F	gaattcgtcataatctttaatttgaaaagatttaaggc	*E. faecalis* Mutant Generation – RNA promoter
oHG186_RNAP-F_citHgRNA1	acaagagtagaaatt**tcattggatcgcctttagcaaag**atctacaagagtagaaattatggtggaatg	*E. faecalis* Mutant Generation – RNA promoter-gRNA(*citH*)
oHG187_citH_ upstream_F	gagcatatggatatgaatttctactcttgtagattctggaaactctcctgctg	*E. faecalis* Mutant Generation – citH upstream homology
oHG188_citH_ upstream_R	gtttttcttcctttctttttagaacttttttg	*E. faecalis* Mutant Generation – citH upstream homology
oHG207_citO_ downstream_F	aaaaagaaaggaagaaaaacgcaaaaaagacctgcagtcg	*E. faecalis* Mutant Generation – citO downstream homology
oHG192_citO_ downstreamflank_R	gcatgtctgcaggcctcgaggatggttactacttagtccaaatg	*E. faecalis* Mutant Generation – citO downstream homology
oHG219_citHflanklong_F	gcaacttcttttgcttctgg	*E. faecalis* Mutant Generation – citHO KO confirmation
oHG192_citO_ downstreamflank_R	gcatgtctgcaggcctcgaggatggttactacttagtccaaatg	*E. faecalis* Mutant Generation – citHO KO confirmation
oHG310_BstXIRD_ RNAP_F	aataaaaagatgccagtgtggtgctggaattcgtcataatctttaatttg	*E. faecalis* Mutant Generation – RNA promoter
oHG311_pflB_gRNA_R	aatt**gcttgttctccatttgtcgcctt**atctacaagagtagaaattatggtggaatgataagggtt	*E. faecalis* Mutant Generation – RNA promoter-gRNA(*pflB*)
oHG312_pflB_uphomology_F	caaatggagaacaagcaatttctactcttgtagatcaccgattgtcatcgttacc	*E. faecalis* Mutant Generation – pflB upstream homology

Primer Name	Primer Sequence	Used for
oHG195_pflB_upstreamflank_R	gaagtgtttgcctccttagtt	*E. faecalis* Mutant Generation – pflB upstream homology
oHG313_pflA_downflank_F	aactaaggaggcaaacacttccaaacgaaaaaatagaaaagaagac	*E. faecalis* Mutant Generation – pflA downstream homology
oHG314_pflA_downhomology_BstXIRD_R	cgatgacgaattccagcacagtcttcttgtgtgcaagttggtg	*E. faecalis* Mutant Generation – pflA downstream homology
oHG315_pflB_flankcheck_F	caagtaatggaagtccacgagatg	*E. faecalis* Mutant Generation – pflAB KO confirmation
oHG316_pflA_flankcheck_R	gcatattgtgtttcttcacttggtg	*E. faecalis* Mutant Generation – pflAB KO confirmation
oHG300_orf19.1117_uphomologySAT1_fwd	gatatctctatttgattgataaaaataacaacttcaacaactactacaacaacaacttaacaacacaaaactagtgaattcgcgctcgag	*C. albicans* Δ*orf19.1117* Generation – homology flanked repair template
oHG301_orf19.1117_downhomologySAT1_rev	gatatttatttaaaaatcaacactataaataaataaaaaacactaatcacataaagatcattgaggttgccgctctagaactagtggatc	*C. albicans* Δ*orf19.1117* Generation – homology flanked repair template
oHG329_orf19.1117_gRNA_primer	cttgcgtaaactatttttaatttg**ggtcaacagtccattctaag**gttttagagctagaaatagca	*C. albicans* Δ*orf19.1117* Generation – PSNR fragment 2
oHG303_orf19.1774_uphomologySAT1_fwd	attgatataacttcattgaattaacaaaccaacaactataataacaactttgacaaacaaacaagcaaaactagtgaattcgcgctcgag	*C. albicans* Δ*orf19.1774* Generation – homology flanked repair template
oHG304_orf19.1774_downhomologySAT1_rev	aatagataaataatactatgaatgaagtgtaaactagccacctttgaggtatttttggttgttgttagccgctctagaactagtggatc	*C. albicans* Δ*orf19.1774* Generation – homology flanked repair template
oHG305_orf19.1774_gRNA_primer	cttgcgtaaactatttttaatttg**agaatccagattattaggta**gttttagagctagaaatagca	*C. albicans* Δ*orf19.1774* Generation – PSNR fragment 2
oHG306_FDH1_uphomologySAT1_fwd	atattaattgattgacaactacaactttatatcaaaccaactaaatcaaaaagcttaacgaaaaacaaaactagtgaattcgcgctcgag	*C. albicans* Δ*FDH1* Generation – homology flanked repair template
oHG307_FDH1_downhomologySAT1_rev	accgtgagatacataacgtttttttagctaaaaaacaaagaaacataatcaaacaagccagctaggattaccgctctagaactagtggatc	*C. albicans* Δ*FDH1* Generation – homology flanked repair template
oHG308_FDH1_gRNA_primer	cttgcgtaaactatttttaatttg**attggttactactactgata**gttttagagctagaaatagca	*C. albicans* Δ*FDH1* Generation – PSNR fragment 2

Table 2.5: Primers Used in RT-qPCR Assays

Primer Name	Primer Sequence	RT-qPCR Target
oHG238_cit1_qpcr_F	CTGACGCCCAAACTAAGGCT	*C. albicans CIT1*
oHG239_cit1_qpcr_R	TTGGGTGCAAGTGAGATGGA	*C. albicans CIT1*
oHG272_fdh_ qpcr _F	TCGCTGCCATTGAAGTTACTG	*C. albicans FDH1*
oHG273_fdh_ qpcr _R	AGCTTGTGCATGTCCTTCACC	*C. albicans FDH1*
oHG76_IRR1_qpcr_F	TCTTGCCTGCTTTGACATGC	*C. albicans IRR1*
oHG77_IRR1_qpcr_R	GCGCTGTTCGTCCTTTTCAA	*C. albicans IRR1*
oHG72_orf19.6843_qpcr_F	ACGGAGATGGGGAGGAAGAA	*C. albicans ORF19.6843*
oHG73_orf19.6843_qpcr_R	TCCCAAGCAACCTCAAAATCAC	*C. albicans ORF19.6843*
oHG280_citH_ qpcr _F	TTTTTGCTGCTGGCGTCTTC	*E. faecalis citH*
oHG281_citH_ qpcr _R	AGCGCCGGCTAATTGTTTTG	*E. faecalis citH*
oHG234_citO_ qpcr _F	AAACATTAGTCGGACGCCCA	*E. faecalis citO*
oHG235_citO_ qpcr _R	ACCACGATACCCACCATAGG	*E. faecalis citO*
oHG250_Ef_rpoB_qpcr_F	ACCAACCGTGAAACAGGTGA	*E. faecalis rpoB*
oHG251_Ef_rpoB_qpcr_R	ATAACACGTTCTGCCCCGTT	*E. faecalis rpoB*
oHG246_Ef_dnaA_qpcr_F	AACCAAATGGCTCATGCTGC	*E. faecalis dnaA*
oHG247_Ef_dnaA_qpcr_R	TCCCTAACCCTACACCACCA	*E. faecalis dnaA*

References

Andrews, S. (2010). *FastQC: a quality control tool for high throughput sequence data*. https://www.bioinformatics.babraham.ac.uk/projects/fastqc/

Chen, S., Zhou, Y., Chen, Y., & Gu, J. (2018). fastp: an ultra-fast all-in-one FASTQ preprocessor. *Bioinformatics*, *34*(17), i884–i890. https://doi.org/10.1093/bioinformatics/bty560

Chua, M. J., & Collins, J. (2022). Rapid, Efficient, and Cost-Effective Gene Editing of Enterococcus faecium with CRISPR-Cas12a. *Microbiology Spectrum*, *10*(1), e02427-21. https://doi.org/10.1128/spectrum.02427-21

Danecek, P., Bonfield, J. K., Liddle, J., Marshall, J., Ohan, V., Pollard, M. O., Whitwham, A., Keane, T., McCarthy, S. A., Davies, R. M., & Li, H. (2021). Twelve years of SAMtools and BCFtools. *GigaScience*, *10*(2), giab008. https://doi.org/10.1093/gigascience/giab008

Dobin, A., Davis, C. A., Schlesinger, F., Drenkow, J., Zaleski, C., Jha, S., Batut, P., Chaisson, M., & Gingeras, T. R. (2013). STAR: ultrafast universal RNA-seq aligner. *Bioinformatics*, *29*(1), 15–21. https://doi.org/10.1093/bioinformatics/bts635

Fozo, E. (2020). *Ef_electocomp_cells_OG1RF*. Protocols.io. https://protocols.io/view/ef-electocomp-cells-og1rf-bp2zmqf6

Gause, H. (2022). *RNA Extraction from Cecum Contents of Gnotobiotic Mice* . Protocols.io. https://www.protocols.io/view/rna-extraction-from-cecum-contents-of-gnotobiotic-5jyl8jjx7g2w/v1/metadata

Harrison, P. W., Amode, M. R., Austine-Orimoloye, O., Azov, A. G., Barba, M., Barnes, I., Becker, A., Bennett, R., Berry, A., Bhai, J., Bhurji, S. K., Boddu, S., Lins, P. R. B., Brooks, L., Ramaraju, S. B., Campbell, L. I., Martinez, M. C., Charkhchi, M., Chougule, K., Cockburn, A., Davidson, C., Silva, N. H. D., Dodiya, K., Donaldson, S., Houdaigui, B. E., Naboulsi, T. E., Fatima, R., Giron, C. G., Genez, T., Grigoriadis, D., Ghattaoraya, G. S., Martinez, J. G., Gurbich, T. A., Hardy, M., Hollis, Z., Hourlier, T., Hunt, T., Kay, M., Kaykala, V., Le, T., Lemos, D., Lodha, D., Marques-Coelho, D., Maslen, G., Merino, G. A., Mirabueno, L. P., Mushtaq, A., Hossain, S. N., Ogeh, D. N., Sakthivel, M. P., Parker, A., Perry, M., Piližota, I., Poppleton, D., Prosovetskaia, I., Raj, S., Pérez-Silva, J. G., Salam, A. I. A., Saraf, S., Saraiva-Agostinho, N., Sheppard, D., Sinha, S., Sipos, B., Sitnik, V., Stark, W., Steed, E., Suner, M.-M., Surapaneni, L., Sutinen, K., Tricomi, F. F., Urbina-Gómez, D., Veidenberg, A., Walsh, T. A., Ware, D., Wass, E., Willhoft, N. L., Allen, J., Alvarez-Jarreta, J., Chakiachvili, M., Flint, B., Giorgetti, S., Haggerty, L., Ilsley, G. R., Keatley, J., Loveland, J. E., Moore, B., Mudge, J. M., Naamati, G., Tate, J., Trevanion, S. J., Winterbottom, A., Frankish, A., Hunt, S. E., Cunningham, F., Dyer, S., Finn, R. D., Martin, F. J., & Yates, A. D. (2023). Ensembl 2024. *Nucleic Acids Research*, *52*(D1), D891–D899. https://doi.org/10.1093/nar/gkad1049

Hernday, A. D., Noble, S. M., Mitrovich, Q. M., & Johnson, A. D. (2010). Chapter 31 Genetics and Molecular Biology in Candida albicans. *Methods in Enzymology*, *470*, 737–758. https://doi.org/10.1016/s0076-6879(10)70031-8

Lee, C., & Johnson, A. (2024). CRISPR/Cas9 genome editing in Candida albicans. *Protocols.Io*. dx.doi.org/10.17504/protocols.io.3byl4we1rvo5/v1

Liao, Y., Smyth, G. K., & Shi, W. (2014). featureCounts: an efficient general purpose program for assigning sequence reads to genomic features. *Bioinformatics*, *30*(7), 923–930. https://doi.org/10.1093/bioinformatics/btt656

Love, M. I., Huber, W., & Anders, S. (2014). Moderated estimation of fold change and dispersion for RNA-seq data with DESeq2. *Genome Biology*, *15*(12), 550. https://doi.org/10.1186/s13059-014-0550-8

Murray, B. E., Singh, K. V., Ross, R. P., Heath, J. D., Dunny, G. M., & Weinstock, G. M. (1993). Generation of restriction map of Enterococcus faecalis OG1 and investigation of growth requirements and regions encoding biosynthetic function. *Journal of Bacteriology*, *175*(16), 5216–5223. https://doi.org/10.1128/jb.175.16.5216-5223.1993

Nguyen, N., Quail, M. M. F., & Hernday, A. D. (2017). An Efficient, Rapid, and Recyclable System for CRISPR-Mediated Genome Editing in Candida albicans. *MSphere*, *2*(2), 10.1128/mspheredirect.00149-17. https://doi.org/10.1128/mspheredirect.00149-17

Skrzypek, M., Binkley, J., Binkley, G., Miyasato, S., Simison, M., & G, S. (n.d.). *Candida Genome Database (CGD)*. Retrieved March 1, 2020, from http://www.candidagenome.org/

Tuch, B. B., Mitrovich, Q. M., Homann, O. R., Hernday, A. D., Monighetti, C. K., Vega, F. M. D. L., & Johnson, A. D. (2010). The Transcriptomes of Two Heritable Cell Types Illuminate the Circuit Governing Their Differentiation. *PLoS Genetics*, *6*(8), e1001070. https://doi.org/10.1371/journal.pgen.1001070

Turnbaugh, P. J., Ridaura, V. K., Faith, J. J., Rey, F. E., Knight, R., & Gordon, J. I. (2009). The Effect of Diet on the Human Gut Microbiome: A Metagenomic Analysis in Humanized Gnotobiotic Mice. *Science Translational Medicine*, *1*(6), 6ra14-6ra14. https://doi.org/10.1126/scitranslmed.3000322

Chapter 3

Results

Transcriptional Response of *C. albicans* to *E. faecalis* in Gut-like *in vitro* Conditions

To determine how *Candida albicans* responds to the presence *of Enterococcus* faecalis (and vice versa), we employed a dual RNA-seq approach. Total RNA was collected from monocultures of *C. albicans* or *E. faecalis* and co-cultures of both species grown in Brain Heart Infusion (BHI) broth for 4 hours in low-oxygen (0.2% O_2) (Figure 3.1A). BHI media was used as it is a rich, complex media that can maintain high intestinal diversity *in vitro* and is a suitable growth medium for *C. albicans* and *E. faecalis* individually (Fox et al., 2014; Yousi et al., 2019). The lumen of the human colon is estimated to have an oxygen content between 0.4-1% (Singhal & Shah, 2020); 0.2% oxygen was used in this study as it was the most relevant condition to mimic the hypoxic environment of the colon while also promoting the growth of both *C. albicans* and *E. faecalis.* Co-culture reads were mapped onto a concatenated *C. albicans-E. faecalis* genome simultaneously to decrease incorrect cross-species mapping, while *C. albicans* only cultures were mapped only to the *C. albicans* genome. We began by analyzing the *C. albicans* expression data and will explore the *E. faecalis* data further on in the manuscript. After trimming and quality filtering, an average of $2.5x10^7$ reads were mapped onto the genome(s) per sample. In *C. albicans* mono-cultures, 86% of those reads were assigned to annotated features, while 9% of the mapped reads in the *C. albicans-E. faecalis* co-culture were assigned to *C. albicans* features.

We defined differentially expressed genes as those with a minimum 4-fold change in gene-expression (adjusted p-value (padj) < 0.05) between *C. albicans* grown in the presence of *E. faecalis* compared to *C. albicans* grown by itself. We observed that *C. albicans* undergoes massive transcriptional changes in the presence of *E. faecalis*, with 230 genes up-regulated at least four-fold and 367 genes down-regulated at least four-fold (Figure 3.1B). Using an

even higher threshold, we observed 82 and 98 genes were up- and down-regulated, respectively, at least eight-fold in the presence of *E. faecalis* in these *in vitro* conditions, further highlighting the dramatic transcriptional change of *C. albicans* in response to *E. faecalis*.

GO term analysis revealed that the genes up-regulated by *C. albicans* in response to *E. faecalis* are enriched for enzymes of the formaldehyde oxidation pathway. The genes down-regulated in response to *E. faecalis* were enriched for genes belonging to pathways including glycolysis and gluconeogenesis, ergosterol biosynthesis, amino acid metabolism and biosynthesis, and translation (Figure 3.1C). As detailed below, we focused our attention on a small number of large changes and followed these up by direct experiments.

Transcriptional Response of C. albicans to E. faecalis in the Gut Microbiome

Not surprisingly, the *C. albicans* gene expression profile *in vitro* and in the mammalian gut are distinct (Rosenbach et al., 2010). To account for the impact of the host in our mixed microbial cultures, we transcriptionally profiled the response of *C. albicans* to *E. faecalis* during growth in the gut of gnotobiotic mice. A minimum of 8 C57BL/6 mice were orally gavaged with either *C. albicans* alone, *E faecalis* alone, or with a mix of both species (Figure 3.2A). Mice were colonized for 10 days and colonization was monitored by plating fecal pellets at 3 and 10 days. At day 10, colonization levels of *E. faecalis* were not significantly different between mono and co-colonized mice; however, the burden of *C. albicans* in the co-colonized mice was significantly lower at day 10 compared to mice colonized with *C. albicans* alone (Supplementary Figure 3.1), indicating that the colonization of *C. albicans* is reduced in the presence of *E. faecalis*.

The ceca of the colonized mice were collected on day 10 and the cecum contents were used to extract total RNA. After filtering low-quality reads, an average of $5.5x10^7$ reads per sample were used as input for genome(s) alignment, and $2.8x10^7$ reads per sample (52%) were uniquely mapped onto the genome(s). The low mapping percentage is unsurprising given the high complexity of the cecum content samples. 75% and 3% of mapped reads were assigned to *C. albicans* features in mono- and co-colonized mice, respectively.

To determine how similar the *C. albicans* transcriptional profile was *in vitro* compared to the mouse gut, Principle Component Analysis (PCA) was performed on all samples. PCA revealed that the first principle component (PC1) was driven by the environment of the experiment; that is, a majority (59%) of the variance seen across all samples can be explained by whether the cells were growing *in vitro* or in the mouse gut (Figure 3.2C). The second principle component (PC2), representing the second largest source of variance (14%), separates the samples by whether *C. albicans* was grown in the presence or absence of *E. faecalis*. Importantly, the PCA analysis revealed a tight clustering within samples grown in the same environment and condition (e.g. *C. albicans* grown alone in the mouse gut), and distinct separation between different sample groups. This analysis demonstrates a high reproducibility of *C. albicans* expression within a group, with the expression profile of each group being distinct from the other groups.

For mouse colonized samples, differentially expressed genes are defined as those *C. albicans* genes with at least 3-fold significant change (padj < 0.05) in expression in the presence of *E. faecalis* compared to growth by itself. We chose this lower threshold because the sequencing depth in the mouse experiments is lower than that *in vitro*. As we observed *in vitro*, the gene expression of *C. albicans* in the mouse gut is significantly impacted by the

presence of *E. faecalis*; 156 and 801 genes are significantly up- and down-regulated, respectively, in the presence of *E. faecalis* (Figure 3.2B).

When comparing the response of *C. albicans* to *E. faecalis* in the mouse gut to that *in vitro*, there is significantly more overlap than one would expect by chance ($p = 2e^{-21}$). 34 genes are up-regulated and 130 genes are down-regulated by *C. albicans* in both *in vitro* and the mouse gut in the presence of *E. faecalis* (Figure 3.2B, Figure 3.2D-E). More than half of the 34 up-regulated genes are uncharacterized in *C. albicans*, including 8 previously identified novel transcripts (nTARs) (Tuch et al., 2010). The 130 down-regulated genes are over-represented for pathways including glycolysis and gluconeogenesis, and acetyl-CoA generation from pyruvate.

Transcriptional Profiling of *E. faecalis* during growth with *C. albicans*

Our RNA extraction protocols and library preparations were designed to sequence RNA from both *C. albicans* and *E. faecalis*, and we could therefore simultaneously examine how *E. faecalis* responds to *C. albicans* in the same co-cultures discussed above. As with *C. albicans*, *E. faecalis* drastically changes its gene expression in response to growth with *C. albicans in vitro*: 249 genes are up-regulated, and 153 genes are down-regulated at least 4-fold in presence of *C. albicans* (Supplementary Figure 3.2). As described below, we focused our work on a specific up-regulated operon. In the mouse gut, we observed little to no effect of *C. albicans* on *E. faecalis* gene expression. We believe this is a reflection of our experimental setup, as the mouse experiments were designed primarily to capture the response of *C. albicans* to *E. faecalis*, so we used a gavage ratio and time point that produced a large excess (10^5) of *E. faecalis* relative to *C. albicans* (Supplementary Figure 3.1). At these ratios, it is

likely the Candida are not abundant enough to induce extensive changes in gene expression in *E. faecalis*.

Up-regulation of *E. faecalis* citrate fermentation during co-culture growth

One of the most highly upregulated pathways in *E. faecalis* in response to *C. albicans* is citrate fermentation. In *E. faecalis*, citrate is metabolized in a two-step process: citrate lyase complex first converts citrate into oxaloacetate, which is then further converted by oxaloacetate decarboxylase enzyme into pyruvate (Figure 3.3A). All the enzymes responsible for citrate metabolism are organized into the *cit* operon, including *citO*, a transcriptional activator of the operon, and *citH*, a citrate specific transporter. When citrate is present, it is imported into the cell via CitH, after which it binds and activates CitO, which triggers a positive feedback loop that further induces the expression of *citH* and *citO* (as well as all the metabolic enzymes) (Sarantinopoulos et al., 2001). In the presence of *C. albicans*, this entire *cit* operon is up-regulated more than 10-fold (Figure 3.3B, Supplementary Figure 3.2). In fact, the transporter *citH* (45-fold) and regulator, *citO* (25-fold) are among the top up-regulated genes in *E. faecalis* when grown with *C. albicans in vitro* (Supplementary Figure 3.2). The *cit* operon in *E. faecalis* is repressed by the Carbon Catabolite Repression (CCR) system, in which the transcriptional repressor CcpA is phosphorylated upon the import of preferential Phosphotransferase System (PTS) sugars, leading CcpA to bind and repress the promoters of alternative carbon metabolic pathways, including the *cit* operon (Suárez et al., 2011). c*cpA* is also down-regulated by *E. faecalis* in the presence of *C. albicans,* consistent with the up-regulation of *cit* operon expression (Figure 3.3B).

To confirm that the up-regulation of the citrate operon in *E. faecalis* reflects the consumption of citrate, we measured the expression of *citH* and *citO* via RT-qPCR in BHI without added glucose (BHI-g) and with or without the addition of 0.2% citrate. The expression of *citH* increases in *E. faecalis* grown in BHI-g+citrate conditions relative to BHI-g-citrate conditions (Figure 3.3C), indicating that the presence of citrate in the media induces the expression of the *cit* operon. Filter-sterilized supernatants of these cultures were then used to measure the citrate concentration. The citrate concentration of BHI-g+citrate media drops to undetectable levels after growth with *E. faecalis*, indicating that the citrate is completely consumed (Figure 3.3D). To verify that the *cit* operon is the only mechanism available to *E. faecalis* to consume citrate, we constructed an *E. faecalis* deletion mutant missing the genes responsible for citrate transport and positive regulation of the cit operon (Δ*citHO*). The citrate concentration of a Δ*citHO* mutant strain does not decrease in BHI-g+citrate media, indicating this operon is responsible for *E. faecalis* consumption and metabolism of citrate *(*Figure 3.3D*)*.

Does the metabolism of citrate improve *E. faecalis* growth? To answer this question, we grew WT and Δ*citHO E. faecalis* strains in BHI-g with or without 0.2% citrate. In BHI-g-citrate conditions, the growth curve of the Δ*citHO* strain was indistinguishable from WT growth (Supplemental Figure 3.3). In BHI-g+citrate, however, the WT *E. faecalis* strain was able to grow to a higher OD at saturation than the mutant strain, whose final OD in the BHI-g+citrate condition was similar to that seen in media without any added citrate (Supplemental Figure 3.3). This increased growth of WT *E. faecalis* in added citrate conditions scales with the amount of citrate added, where higher final ODs are observed as the citrate concentration increases (Supplemental Figure 3.3). If glucose is abundant, there

is little effect of added citrate, supporting previous findings that citrate is not a preferred carbon source (Suárez et al., 2011); in the absence of glucose, however, citrate leads to additional growth of *E. faecalis*.

E. faecalis induces the up-regulation of *C. albicans* citrate synthase during co-culture

One of the highest up-regulated *C. albicans* genes in response to *E. faecalis*, both in the mouse gut and in lab conditions, is citrate synthase (*CIT1*). Cit1 is the first enzyme of TriCarboxylic Acid (TCA) cycle and catalyzes the addition of acetyl-CoA to oxaloacetate to produce citrate. While this enzyme is highly induced in the presence of *E. faecalis* (12-fold up-regulated in vitro, 4-fold in the mouse gut), the additional enzymes of the TCA cycle are not up-regulated in a similar fashion (Figure 3.4A). In fact, the TCA enzymes directly downstream of Cit1, Aco1 and Aco2 (which convert citrate to isocitrate) are down-regulated in the presence of *E. faecalis.* Based on these observations, the up-regulation of *CIT1* by *C. albicans* in response to *E. faecalis* does not fit well into a general increase of metabolic flux.

C. albicans CIT1 up-regulation and citrate secretion

What causes *C. albicans* to up-regulate *CIT1* in the presence of *E. faecalis*? We think it is likely that glucose depletion is the signal, based on the following observations. *C. albicans* grown in BHI-g expresses *CIT1* at higher levels than in BHI media with 0.2% glucose (Figure 3.4B). This *CIT1* up-regulation is similar in magnitude to that seen when *C. albicans* is grown in the presence of *E. faecalis*. In addition, the expression of *CIT1* in *C. albicans* grown with the *E. faecalis* Δ*citHO* strain is similar to *CIT1* expression in *C. albicans* is grown with WT *E. faecalis*, indicating that citrate concentration is not the relevant signal (Figure 3.4B).

C. albicans citrate production increases growth capability of *E. faecalis*

Given that, (1) *C. albicans* citrate production is up-regulated in the presence of *E. faecalis*, (2) increased citrate is secreted, and (3) in the presence of *C. albicans*, *E. faecalis* up-regulates the operon responsible for citrate metabolism, we tested whether citrate production by *C. albicans* can support *E. faecalis* growth. In other words, does *E. faecalis* have a fitness advantage when growing with *C. albicans* due to citrate production from the yeast? To answer this question, we grew co-cultures of *C. albicans* and *E. faecalis* in hypoxic conditions in BHI-g +/- 0.2% citrate for 24 hours. When WT *E. faecalis* is grown with a *C. albicans* strain incapable of making citrate (Δ*CIT1*) in BHI-g-citrate, the saturated concentration of *E. faecalis* is significantly lower than that seen when WT *E. faecalis* is grown with WT *C. albicans (*Figure 3.5*)*. Importantly, this difference in final cell concentration between *E. faecalis* grown with WT and Δ*CIT1* strains of *C. albicans* disappears when a Δ*citHO E. faecalis* strain is used. That is, an *E. faecalis* strain incapable of consuming citrate no longer benefits from citrate produced by *C. albicans*. Furthermore, the fitness defect of *E. faecalis* grown with Δ*CIT1 C. albicans* disappears when citrate is added to the media (Figure 3.5). Taken together, these results show that *E. faecalis* is capable of consuming citrate produced by *C. albicans,* and that this consumption leads to a fitness increase for the bacteria during co-culture. While the difference in final cell concentration may be small, it is highly reproducible. Although citrate is one of many nutrients *E. faecalis* is capable of metabolizing, our results show that *CIT1*-intact *C. albicans* provides a growth advantage to *E. faecalis*.

Co-culture induces up-regulation of formate dehydrogenases in *C. albicans*

C. albicans encodes three very similar formate dehydrogenases, *FDH1*, *ORF19.1117*, and *ORF19.1774*. All three formate dehydrogenases (FDHs) were among the top 15 genes up-regulated in the presence of *E. faecalis in vitro* (Figure 3.1A). In fact, one of the formate dehydrogenases, *ORF19.1117*, is the *C. albicans* gene that is most up-regulated (545-fold) in *C. albicans* in response to *E. faecalis* (Figure 3.1A). In the mouse gut, the *Candida* FDH1 gene is up-regulated by the presence of *E. faecalis*; expressed; read counts for the other two FDHs did not pass filtering thresholds and were therefore not able to be evaluated.

Formate dehydrogenases are a class of enzyme that catalyze the oxidation of formate into CO_2, reducing NAD+ to NADH in the process. Given the high-magnitude up-regulation of all three of the *C. albicans* FDHs in the presence of *E. faecalis in vitro*, we hypothesized that formate itself produced by *E. faecalis* could be the inducer. When *E. faecalis* ferments citrate, it is known to produce formate and acetate, among other minor downstream products (Sarantinopoulos et al., 2001) (Figure 3.6B). Given that citrate fermentation is increased in *E. faecalis* on exposure to *C. albicans*, we first determined whether this lead to an increase in extracellular formate concentration. WT *E. faecalis* cultured in BHI-g for 24 hours produce approximately 0.5 g/L of formate (Figure 3.6D) . When the media is supplemented with 0.2% citrate, formate concentration for WT *E. faecalis* cultures increases to 0.85 g/L (Figure 3.6D). If *E. faecalis* is unable to utilize citrate (that is, when *citHO* is deleted), it produces significantly less formate than the WT strain in the presence of citrate (Figure 3.6D). In addition to the *citHO* genes, the production of formate by *E. faecalis* is dependent on the expression of the downstream pyruvate formate lyase (PFL) (*pflA* and *pflB*), as a mutant

strain of *E. faecalis* deleted for both PFL enzymes (Δ*pflA*/Δ*pflB*) is deficient for formate secretion (Figure 3.6D).

An important role of formate dehydrogenases in fungi is to detoxify formate (Maier et al., 2024). The toxic effect of formate is through binding and inhibiting cytochrome c, the terminal electron acceptor of the electron transport chain (Nicholls, 1975). To test whether the *C. albicans* FDH enzymes are protective against formate, we constructed *C. albicans* mutants missing one, two, or all three of the FDH genes. In BHI-glucose media with 4% formate, *C. albicans* missing all three FDH enzymes (FDH3Δ) had a lower final OD at saturation than WT or strains missing one or two FDH enzymes (Figure 3.6C), indicating that the FDH genes lead to increased fitness in the presence of formate.

Is detoxification of formate the major role of the FDH's when *C. albicans* is cultured with *E. faecalis*? Some fungal species can utilize formate as a carbon source via C1-tetrahydrofolate (THF) synthase, which catalyzes the three sequential reactions that convert formate and THF to methylene-THF. Intermediates of these reactions are precursors for many metabolic processes, including purine and amino acid biosynthesis (Appling & Rabinowitz, 1985). Although this reaction has not been extensively studied in *C. albicans*, this species encodes two homologs of known C1-THF synthases (*MIS11* and *MIS12*). However, both of these homologs are down-regulated in the presence of *E. faecalis*, indicating that *C. albicans* is not using formate as a carbon source in the presence of *E. faecalis* (Figure 3.6A). Rather we conclude that the main role of FDH up-regulation by *C. albicans* in the presence of *E. faecalis* is to detoxify formate produced by metabolism of citrate by the bacterium.

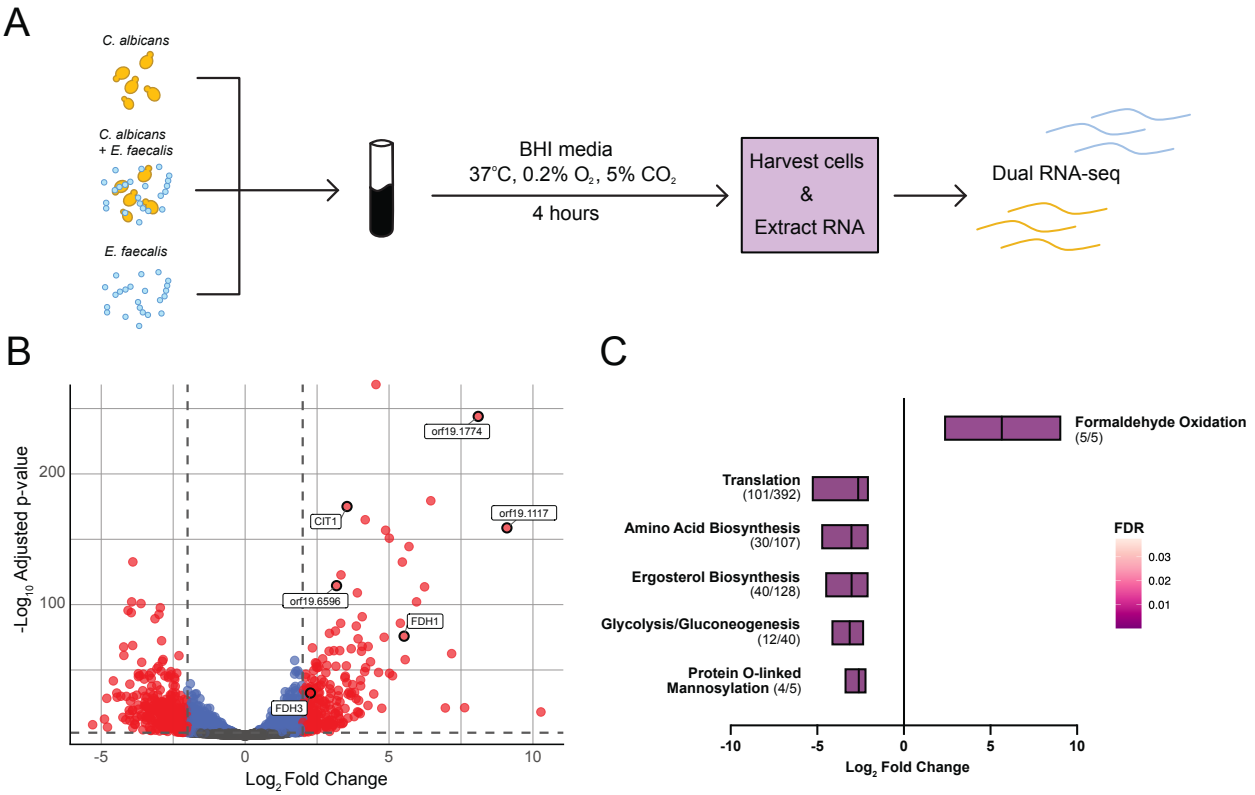

Figure 3.1 *in vitro* Profiling of *Candida albicans* Gene Expression Response to *Enterococcus faecalis* A) Schematic of *in vitro* Dual RNA-seq experiment with *C. albicans* and *E. faecalis* grown in mono-culture or co-culture in 0.2% O_2, 5% CO_2, and 37°C conditions. B) Volcano plot of *C. albicans* gene expression during growth with *E. faecalis* compared to growth by itself. Each point represents a *C. albicans* single gene. Induced genes are on the right of the plot, repressed genes are on the left of the plot. Genes with significant differential expression are color-coded: red dots for genes with over 4-fold change (adjusted p-value < 0.05), blue dots for genes with significant but less than 4-fold change, and grey dots for non-significant changes. Labeled dots correspond to genes belonging to the formaldehyde oxidation pathway or *CIT1*, a gene discussed in more detail later in the chapter. C) Pathway enrichment plot for significantly up- and down-regulated genes in *C. albicans* in the presence of *E. faecalis* compared to *C. albicans* by itself. Up-regulated pathways are on the right of the plot and down-regulated pathways are on the left of the plot. Titles of the enriched pathways are next to bars representing the minimum and maximum Log_2 fold-change of the pathway, with the middle line representing the average Log_2 fold-change in expression of the pathway. The color of the bar represents the False Discovery Rate (FDR) of over-representation for a given pathway. In parentheses below pathway titles is the number of genes up- or down-regulated over the total number of genes in the pathway.

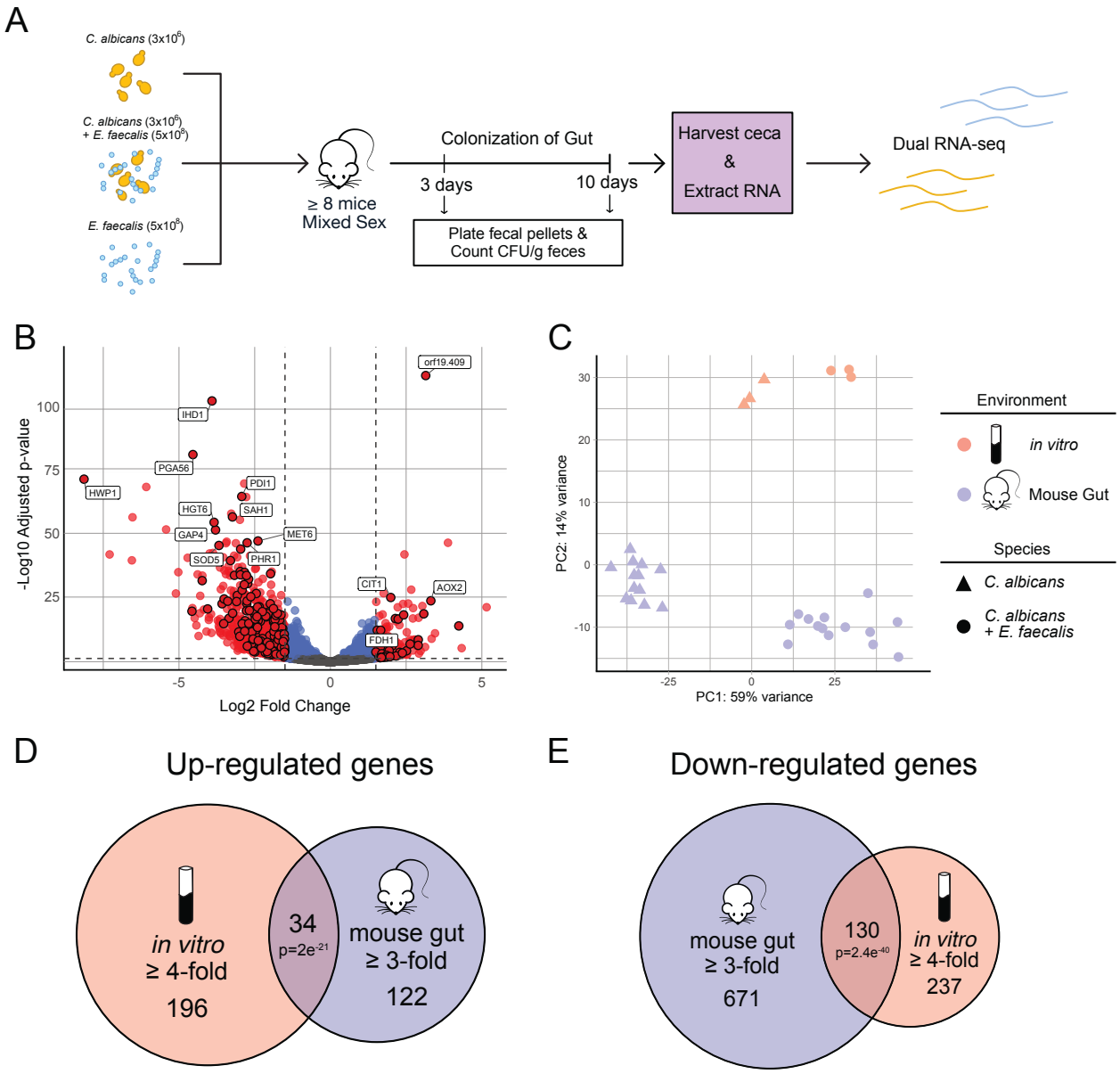

Figure 3.2 *C. albicans* Gene Expression Response to *E. faecalis* in the Gut Microbiome
(A) Schematic representation of germ-free mouse colonization with either *Candida albicans* or *Enterococcus faecalis* alone or both species together to examine RNA-seq profiles. **(B)** Volcano plot illustrating *C. albicans* gene expression changes during colonization of the mouse gut with *E. faecalis* compared to *C. albicans* alone. Genes with significant differential expression are color-coded: red dots for genes with over 4-fold change (adjusted p-value < 0.05), blue dots for genes with significant but less than 4-fold change, and grey dots for non-significant changes. Genes also differentially expressed in the same direction in response to *E. faecalis* in vitro are highlighted with black outlines, with a subset labeled for identification.**(C)** Principal Component Analysis (PCA) plot showing RNA-seq expression results for *C. albicans* grown alone (triangles) or with *E. faecalis* (circles) in either mouse gut (purple) or *in vitro* (peach) conditions; results are projected onto the first two principal components (PC1 and PC2) to represent (Figure caption continued on the next page.)

(Figure caption continued from the previous page.) the major patterns of variation within the dataset. Each dot represents a single sample, and positions of the dots indicate their relative similarity or dissimilarity. Tight clustering within group indicates high intra-group similarity while separation between groups indicates inter-group differences in gene expression. D&E) Venn diagram displaying the overlap between up- (D) and down-regulated (E) *C. albicans* genes induced in the presence of *E. faecalis*. Significance of overlap indicated by p-value generated by a hypergeometric test with a total population size of 6200 genes.

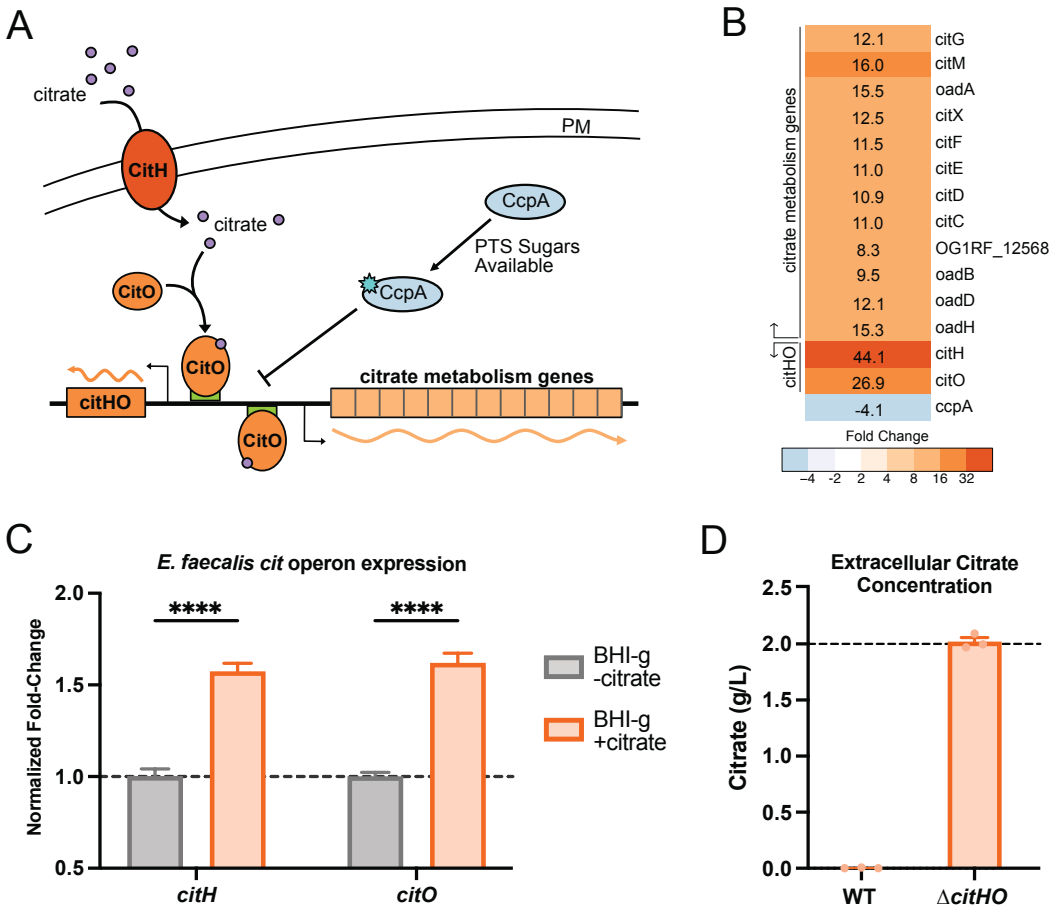

Figure 3.3 *E. faecalis* Up-regulates Citrate Metabolism in Presence of *C. albicans*
A) Diagram depicting regulation of the *cit* operon in *E. faecalis*. After import into the cell via CitH, citrate binds the transcriptional activator CitO, which permits binding of regulatory regions upstream of the transcription start sites of *citHO* and *citCL*, the two halves of the bi-directional *cit* operon. CcpA acts as a transcriptional repressor of the *cit* operon when preferential Phosphotransferase System (PTS) sugars are present. Color of proteins and operon gene blocks represent Log_2 Fold Change in presence of *C. albicans* compared to *E. faecalis* alone using scale in panel B. B) Heatmap of Log_2 Fold Change values for *cit* operon and *ccpA* in *E. faecalis* during growth with *C. albicans* compared to growth alone. citM, soluble oxaloacetate decarboxylase; citC, citDEF, citX,and citG, citrate lyase subunits and accessory proteins; citO, transcriptional regulator ; citH, citrate transporter; oadA, oadB , oadD, oadH, and OG1RF_12568 (oadG-like), subunits of the membrane-bound oxaloacetate decarboxylase. Operon organization indicated with vertical labels on the left side. C) RT-qPCR data showing change in expression of *citH* and *citO* in *E. faecalis* when grown in citrate-replete relative to citrate deplete conditions in BHI– glucose media. Bars represent the average of three biological replications, error bars representing standard error. D) Concentration of citrate (g/L) in BHI – glucose + 0.2% citrate media after 4 hours of WT or ΔcitHO *E. faecalis* growth. Dashed line represents the concentration of citrate in media. Bars represent average of three replicates (same samples as shown in panel C), error bars represent standard error.

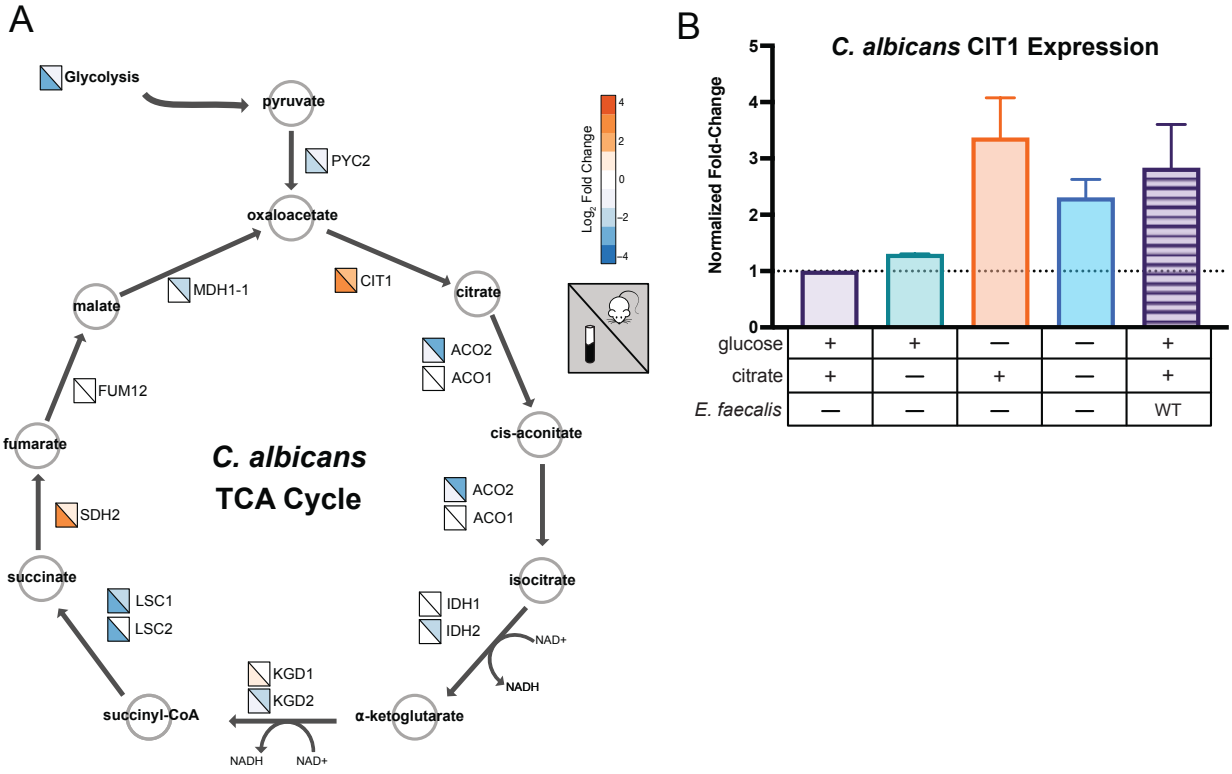

Figure 3.4 *C. albicans* Up-regulates Citrate Production in Presence of *E. faecalis*
A) Diagram depicting the TriCarboxylic Acid (TCA) Cycle in *C. albicans*. Reactions indicated by arrows labeled with the enzyme responsible for that reaction. Box next to enzyme names indicates Log_2 Fold Change in expression in *C. albicans* when grown with *E. faecalis* compared to growth alone. Upper right triangle in box represents fold-change in the mouse gut, lower right triangle represents fold-change *in vitro*. PYC2, pyruvate carboxylase; CIT1, citrate lyase; ACO1 & ACO2, aconitases; IDH1 & IDH2, isocitrate dehydrogenase; KGD1 & KGD2, alpha-ketoglutarate dehydrogenase complex; LSC1 & LSC2, succinyl-CoA ligase subunits; SDH2, succinate dehydrogenase; FUM12, fumarate hydratase; MDH1-1, malate dehydrogenase. B) RT-qPCR results for *C. albicans CIT1* expression in BHI media with different glucose and citrate availabilities, and in the presence of *E. faecalis*, as indicated by the table below the graph. Data shown as the relative fold-change in expression compared to BHI + glucose + citrate condition. Bars represent the average fold-change of 3 biological replicates, error bars represent the standard error.

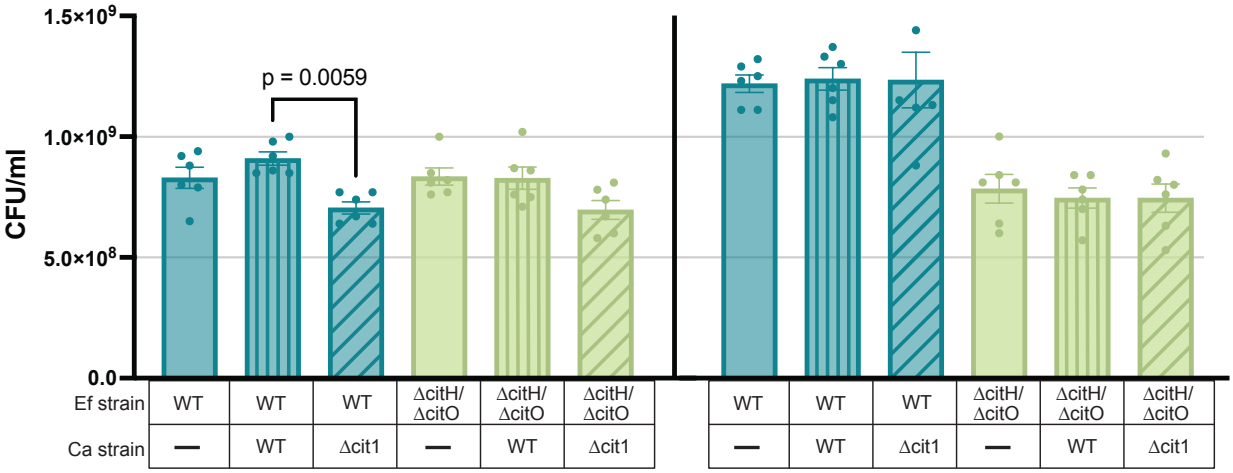

Figure 3.5 *C. albicans* Citrate Production Increases Growth of *E. faecalis*
Barplot representing the concentration (CFU/ml) of *E. faecalis* in mono-culture or co-culture with *C. albicans* after 24 hours of growth in BHI – glucose with (right) or without (left) added 0.2% citrate. In BHI-glucose+citrate, growth of WT *E. faecalis* decreases when co-cultured with ΔCIT1 *C. albicans* mutant compared to growth with WT *C. albicans*. This decrease of growth is not seen in the Δ*citHO E. faecalis* mutant nor seen in WT *E. faecalis* when citrate is added to the media.

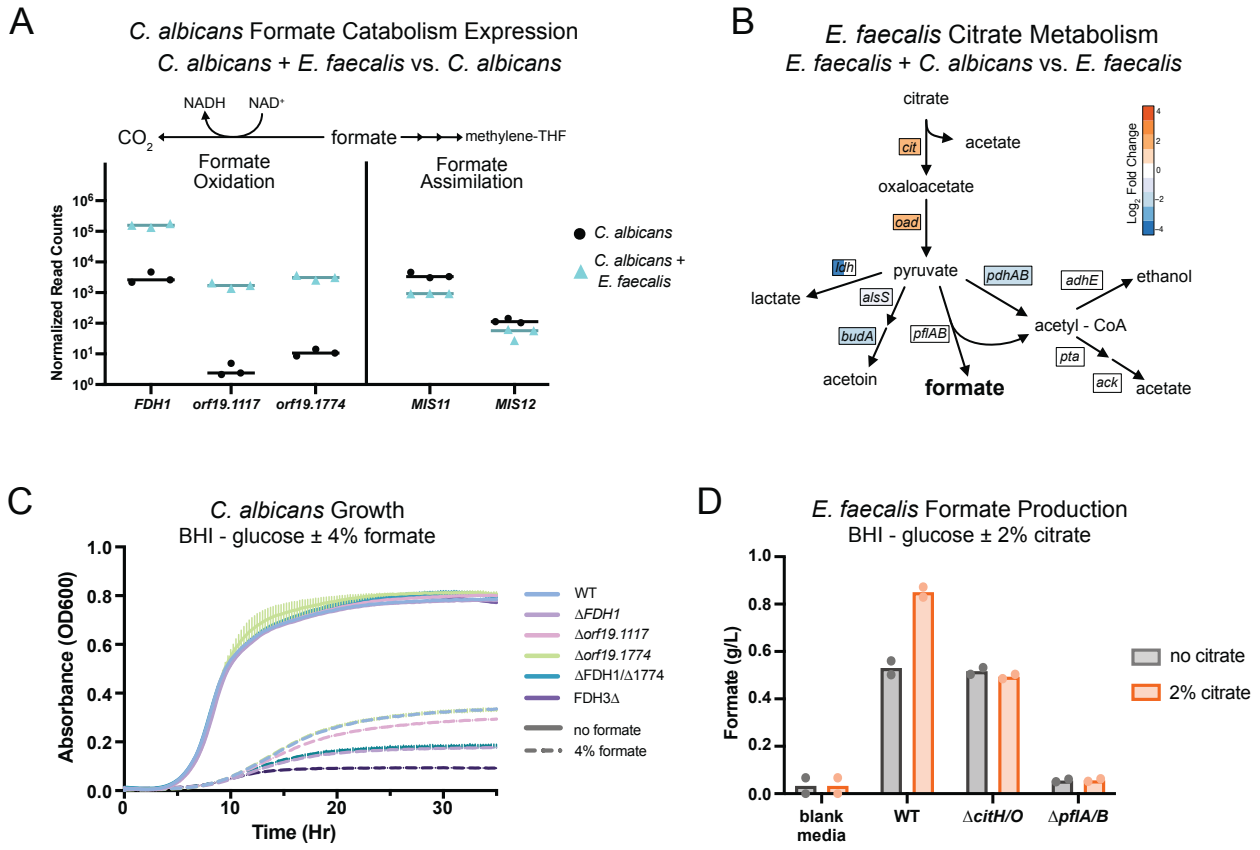

Figure 3.6 *C. albicans* Detoxifies Formate Produced by *E. faecalis*
A) RNA-Seq normalized counts of *C. albicans* genes of formate catabolism enzymes. Simple schematic of each reaction shown above plot. Left: Formate oxidation, FDH genes (FDH1, orf19.1117, orf19.1774), Right: Formate assimilation, C1-THF synthase genes (MIS11, MIS12). Normalized counts of *C. albicans in vitro* mono-cultures (black) and *C. albicans-E. faecalis* co-cultures (blue). B) Diagram of citrate and downstream metabolism. Enzymes catalyzing each reaction boxed next to arrows. Color of box indicates Log_2 fold change in expression of gene in *C. albicans-E. faecalis* co-cultures compared to *E. faecalis* mono-cultures. C) Growth Curve of *C. albicans* strains grown in BHI-glucose with or without 4% formate. Solid line represents cultures without formate, dashed line represents cultures with formate. Color of line represents *C. albicans* WT or FDH deletion mutant. *C. albicans* strain FDH3Δ is a triple deletion for FDH1, orf19.1117, orf19.1774. D) Formate production of *E. faecalis* WT and deletion strains in BHI-glucose with or without added 2% citrate.

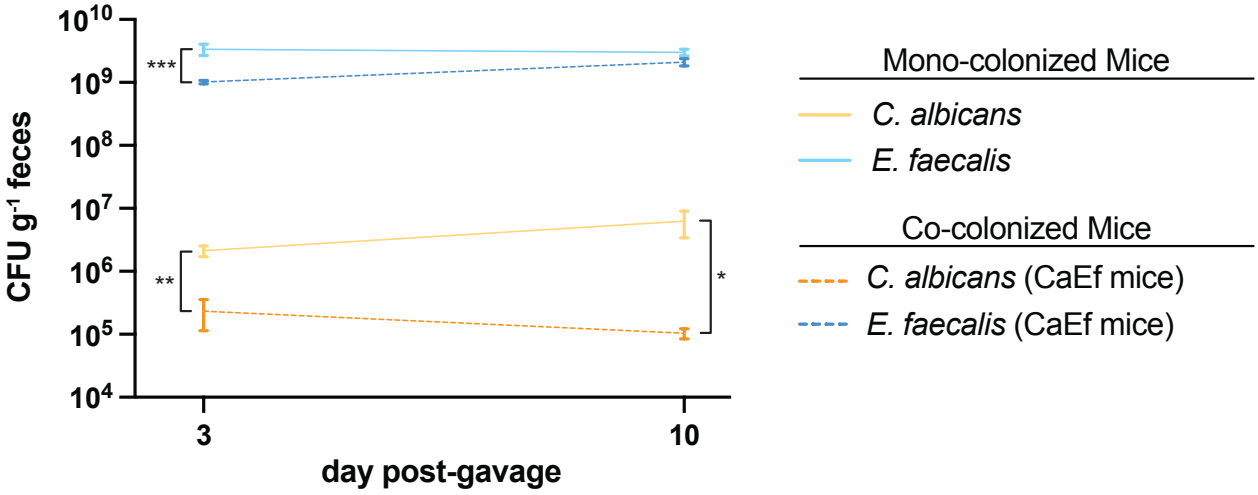

Supplemental Figure 3.1 Microbial Burden of Gnotobiotic Mice Mono-colonized or Co-colonized with *C. albicans* and *E. faecalis*
Concentration of *C. albicans* and *E. faecalis* in fecal pellets of mice collected on either day 3 or day 10. Error bars represent standard error across >8 mice. Point at which line meets error bars represents the mean for each group. Significance determined using student's t-test within each species and time comparison.

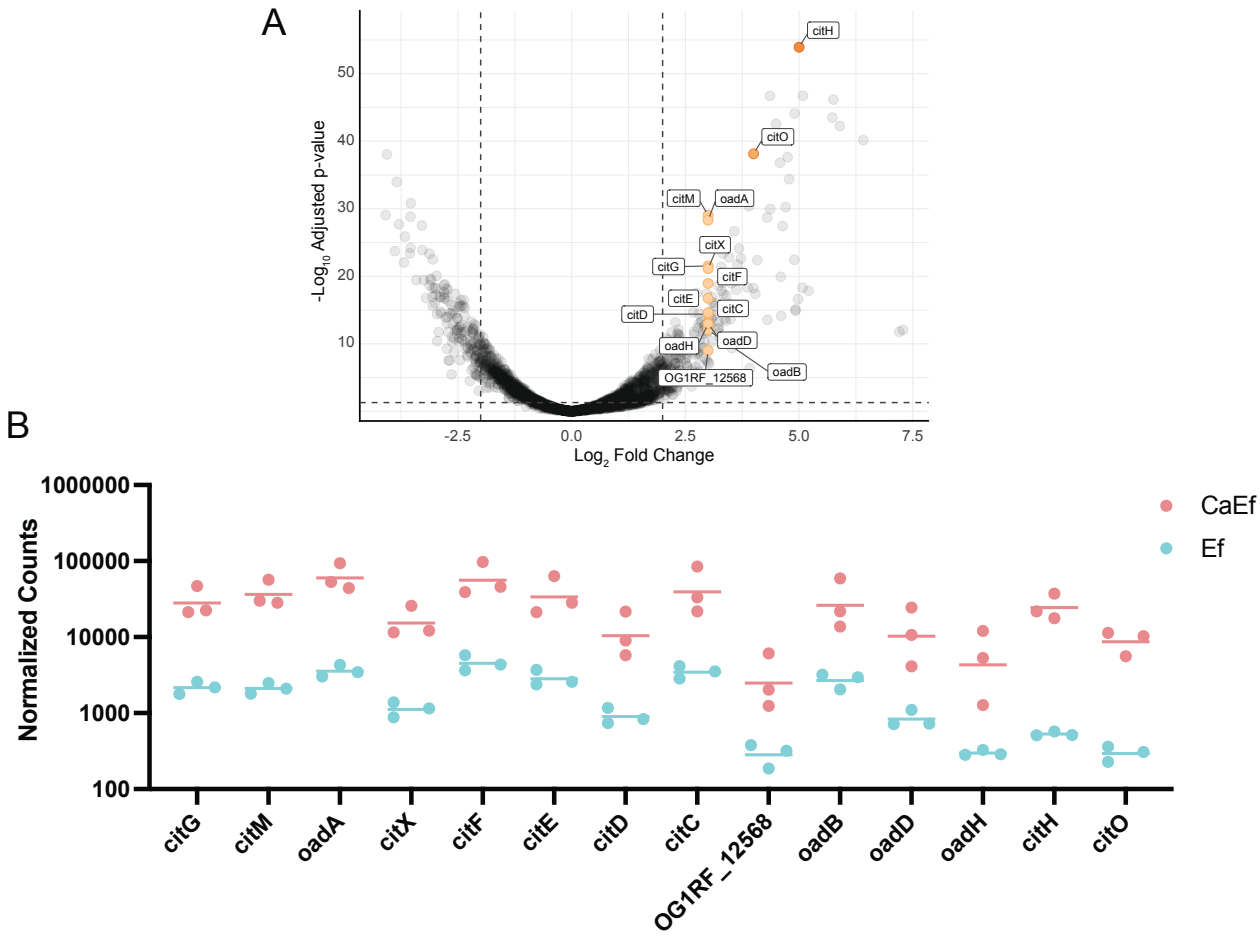

Supplementary Figure 3.2 *E. faecalis* expression of *cit* operon in presence of *C. albicans*

A) Volcano plot showing gene expression changes for all genes of *E. faecalis* during co-culture with *C. albicans in vitro* compared to growth by itself. Colored and labeled dots represent the genes encoded in the *cit operon*. B) Normalized counts for genes encoded in the *cit* operon in *E. faecalis* during co-culture with *C. albicans*. Each dot represents the normalized count of the gene in one sample, with the line representing the average normalized count per group.

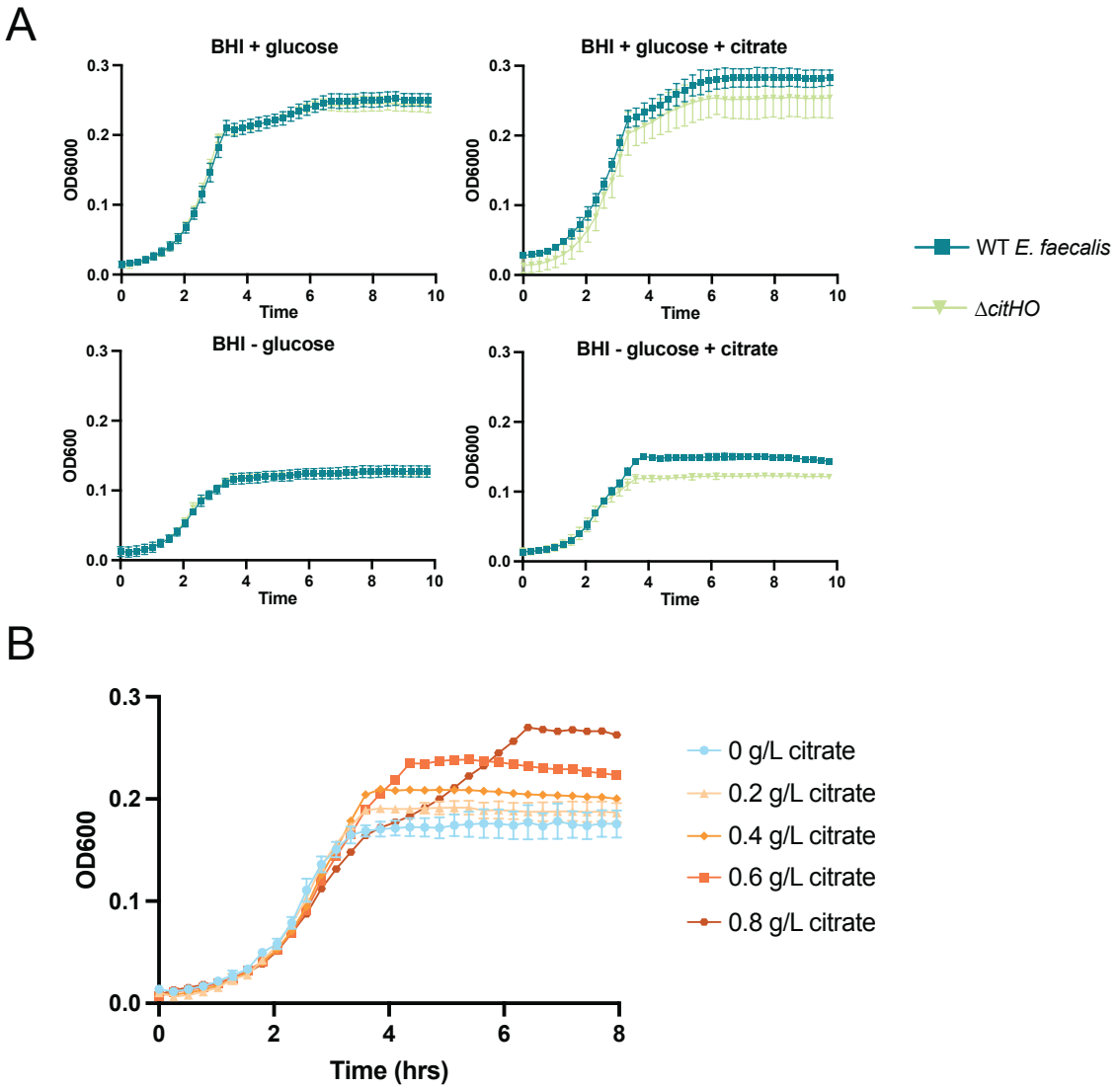

Supplemental Figure 3.3 Citrate metabolism associated with increased growth in *E. faecalis*

A) Growth curves of WT or ΔcitHO *E. faecalis* when grown in BHI media 1) with or without 0.2% glucose, and 2) with or without 0.2% citrate. Growth curves measured on Tecan via absorbance (OD600) in gut-like conditions (0.2% oxygen, 5% CO_2, 37°C.) Each point represents the average of three biological replicate wells with error bars representing standard error. As seen in the lower right plot, a growth advantage is evident for WT *E. faecalis* when grown in no added glucose with added citrate conditions. B) Growth advantage of E. faecalis scales with concentration of citrate present in media. WT *E. faecalis* was grown in BHI - glucose with citrate added at increasing concentrations (0 – 0.8 g/L). Carrying capacity (or OD600 at saturation) of *E. faecalis* increases with higher citrate concentrations.

References

Appling, D. R., & Rabinowitz, J. C. (1985). Regulation of expression of the ADE3 gene for yeast C1-tetrahydrofolate synthase, a trifunctional enzyme involved in one-carbon metabolism. *Journal of Biological Chemistry*, *260*(2), 1248–1256. https://doi.org/10.1016/s0021-9258(20)71236-6

Fox, E. P., Cowley, E. S., Nobile, C. J., Hartooni, N., Newman, D. K., & Johnson, A. D. (2014). Anaerobic Bacteria Grow within Candida albicans Biofilms and Induce Biofilm Formation in Suspension Cultures. *Current Biology*, *24*(20). https://doi.org/10.1016/j.cub.2014.08.057

Maier, A., Mguni, L. M., Ngo, A. C. R., & Tischler, D. (2024). Formate Dehydrogenase: Recent Developments for NADH and NADPH Recycling in Biocatalysis. *ChemCatChem*. https://doi.org/10.1002/cctc.202401021

Nicholls, P. (1975). Formate as an inhibitor of cytochrome c oxidase. *Biochemical and Biophysical Research Communications*, *67*(2), 610–616. https://doi.org/10.1016/0006-291x(75)90856-6

Rosenbach, A., Dignard, D., Pierce, J. V., Whiteway, M., & Kumamoto, C. A. (2010). Adaptations of Candida albicans for Growth in the Mammalian Intestinal Tract ▿ †. *Eukaryotic Cell*, *9*(7), 1075–1086. https://doi.org/10.1128/ec.00034-10

Sarantinopoulos, P., Kalantzopoulos, G., & Tsakalidou, E. (2001). Citrate Metabolism by Enterococcus faecalis FAIR-E 229. *Applied and Environmental Microbiology*, *67*(12), 5482–5487. https://doi.org/10.1128/aem.67.12.5482-5487.2001

Singhal, R., & Shah, Y. M. (2020). Oxygen battle in the gut: Hypoxia and hypoxia-inducible factors in metabolic and inflammatory responses in the intestine. *Journal of Biological Chemistry*, *295*(30), 10493–10505. https://doi.org/10.1074/jbc.rev120.011188

Suárez, C. A., Blancato, V. S., Poncet, S., Deutscher, J., & Magni, C. (2011). CcpA represses the expression of the divergent cit operons of Enterococcus faecalis through multiple cresites. *BMC Microbiology*, *11*(1), 227. https://doi.org/10.1186/1471-2180-11-227

Tuch, B. B., Mitrovich, Q. M., Homann, O. R., Hernday, A. D., Monighetti, C. K., Vega, F. M. D. L., & Johnson, A. D. (2010). The Transcriptomes of Two Heritable Cell Types Illuminate the Circuit Governing Their Differentiation. *PLoS Genetics*, *6*(8), e1001070. https://doi.org/10.1371/journal.pgen.1001070

Yousi, F., Kainan, C., Junnan, Z., Chuanxing, X., Lina, F., Bangzhou, Z., Jianlin, R., & Baishan, F. (2019). Evaluation of the effects of four media on human intestinal microbiota culture in vitro. *AMB Express*, *9*(1), 69. https://doi.org/10.1186/s13568-019-0790-9

Chapter 4

Discussion

Despite many studies implicating individual microbial species in various human health outcomes, the detailed molecular interactions between different microbial species within the gut microbiome have not been extensively studied. Evidence to date suggests that the impact of any particular species on host interactions (e.g. drug metabolism, gut epithelial integrity) can be influenced by the interactions with other community members (Garcia-Santamarina et al., 2024; Gould et al., 2018). Fully understanding the role of a species in the microbiome, therefore, requires unraveling its interactions with other microorganisms of this community. However, the complexity of the adult microbiome presents significant experimental challenges in isolating and studying interactions between different species within this intricate network. In this study, we used the minimally colonized pre-term infant gut microbiome as a starting place to study interactions between two common infant colonizers, the yeast *Candida albicans* and the bacterium *Enterococcus faecalis.* We first examined how the presence of each species affects the other's gene expression profile during growth together in the gut of gnotobiotic mice and *in vitro* conditions designed to mimic several key features of the gut environment. This study reveals that each species greatly influences the gene expression pattern of the other, offering new insights into the interactions between these organisms. As described below, we followed up on several of the most striking observations by developing hypotheses and testing them by direct experimentation.

The environment encountered by microbes in the mammalian gut differs significantly from *in vitro* conditions due to various factors, such as constant nutrient replenishment, interactions with host epithelial cells, and interactions with the immune system (Zeng et al., 2022) Data from our study highlight these environmental differences, revealing that the

effect of *E. faecalis* on *C. albicans* gene expression differs significantly in the gnotobiotic mouse gut compared to our *in vitro* conditions (BHI medium, 37^{o}C, low oxygen) (Figure 2C). Despite these differences, many of the transcriptional changes *C. albicans* undergoes in response to *E. faecalis* in the mouse gut are observed both *in vitro* and *in vivo*. The significant overlap between the two conditions highlights that the core response of *C. albicans* to this bacterium is robust to different conditions. This study strongly supports the idea that even simplified *in vitro* conditions (rich nutrients, body temperature, and low oxygen) are sufficient to investigate interactions between two species of gut microbes. This study also informs an ongoing issue with sequencing depth, long considered a limitation in studying gene expression in vivo (Haas et al., 2012; Zaheer et al., 2018). Our study shows that despite large differences in sequencing depth between the mouse gut and *in vitro* environments, *C. albicans* genes showing substantial expression changes in response to growth with *E. faecalis* can be detected in both high- and low-sequencing depth conditions. The overall result from the reciprocal RNA-seq experiments are summarized in Figure 3.2.

Following up on results from the RNA-seq experiments, we showed that, upon exposure to *E. faecalis*, *C. albicans* up-regulates the production of citrate. If the citrate produced is not feeding the TCA cycle (as evidenced by the down-regulation of downstream enzymes in the cycle), where is it going? Many fungal species are known to secrete citrate; *Aspergillus niger* and *Yarrowia lipolytica* are the main producers of citric acid used in food production (Książek, 2023). Although not to the same degree as industrial citrate producers, *C. albicans* is also known to secrete citrate (0.32-0.41 mM) (Oliver 2020). The secretion of citrate by yeast requires both the up-regulation of *CIT1* and the down-regulation of downstream enzymes of the TCA that would otherwise re-direct the flux of citrate through

the cycle (Carsanba et al., 2019). During co-culture with *E. faecalis*, we observed this regulatory pattern in *C. albicans,* suggesting *C. albicans* is secreting citrate. We also show that glucose depletion is sufficient to upregulate *CIT1* and believe that glucose depletion by *E. faecalis* is the primary signal that triggers up-regulation of *CIT1* in the co-culture conditions. Low-glucose is known to up-regulate the expression of *CIT1* in *Saccharomyces cerevisiae* (Rosenkrantz et al., 1994). Although glucose depletion is the main signal, it is possible other signals contribute to the up-regulation of *CIT1*, as low nitrogen and iron have also been shown to be key signals for other citrate-secreting fungi; these elements are known to be limiting resources in polymicrobial interactions (Fourie et al., 2018; Hattab et al., 2022; Reese et al., 2018).

Transcriptional profiling also revealed that, in the presence of *C. albicans*, *E. faecalis* greatly increased the expression of genes responsible for citrate metabolism. Competitive growth experiments showed that, in the presence of *C. albicans*, *E faecalis* strains capable of metabolizing citrate had a growth advantage over otherwise isogenic *E. faecalis* strains deleted for genes needed to metabolize citrate. This finding is consistent with a recent study showing that *E. faecalis* strains capable of metabolizing citrate exhibited increased growth in blood and urine, as well as heightened virulence in a *Galleria* infection model (Martino et al., 2018). Our work builds on these findings by demonstrating that *E. faecalis* can utilize citrate produced and secreted by *C. albicans*, effectively exploiting this metabolic interaction to enhance its own fitness. Recently, Mould et al. showed that intra- and inter-species cross-feeding of citrate can impact the virulence and fitness of bacteria, (Mould et al., 2024), and the work described here provides the first example of cross-kingdom metabolic cross-feeding of citrate.

Our transcriptional profiling also revealed that the *C. albicans* formate dehydrogenase genes (*FDH1*, *ORF19.1117*, *ORF19.1774*) are highly up-regulated in the presence of *E. faecalis*. Formate, a short-chain fatty acid (SCFA) produced by gut bacteria, is one of the main byproducts of citrate metabolism in *E. faecalis* (Ramsey et al., 2014). SCFAs, such as butyrate or acetate, have been widely studied in recent years due to their role in intestinal epithelial integrity and immune modulation (Mann et al., 2024). While the role of formate in the gut microbiome is less well understood compared to other SCFAs, recent reports indicate that formate concentrations increase in the gut microbiome during dysbiosis in mouse models of colitis (Hughes, 2017). Additionally, this study showed that formate dehydrogenase conferred a fitness advantage to bacteria in the dysbiotic gut.

We hypothesized that in our co-culture experiments, *E. faecalis* metabolizes citrate (provided in part by *C. albicans*) to formate, which is subsequently secreted. This secreted formate then induces the expression of three *C. albicans* formate dehydrogenase genes. Formate is known to be toxic to yeast at high concentrations (Du et al., 2022; Wang et al., 2023), and we further hypothesized the up-regulation of these FDHs is a mechanism for *C. albicans* to detoxify formate produced by *E. faecalis* and other formate-producing bacteria in order to survive in the gut microbiome. We showed that the three FDHs are individually sufficient for tolerating high formate concentrations. *C. albicans*' ability to detoxify formate produced by *E. faecalis* gives the yeast a fitness advantage over non-FDH encoding gut microbes and may in part explain the observed association of these two species during dysbiosis in the gut.

C. albicans and *E. faecalis* are commonly associated microbes in the gut microbiome that, in periods of dysbiosis, rise from low cell numbers in the healthy gut to high

concentrations where they have the potential to translocate from the gut to the bloodstream and cause lethal infection (Archambaud et al., 2019; Daca & Jarzembowski, 2024; Kumamoto et al., 2020; Zhai et al., 2020). Collectively, this work demonstrates an exploitative metabolic cross-feeding interaction between this yeast and a bacterium: *C. albicans* is forced to up-regulate genes to tolerate the toxic byproduct generated by the very metabolic pathway it supports in *E. faecalis*. Citrate metabolism and formate production are ubiquitous among lactic acid and other anaerobic bacteria (Antranikian & Giffhorn, 1987; Hugenholtz, 1993; Pietzke et al., 2020); therefore, the metabolic network presented here may serve as a proxy for the interactions between *C. albicans* and other bacterial members of the gut microbiome and other mucosal sites of colonization. This work reinforces the importance of cross-kingdom metabolic interactions in commensalism and virulence. Even though *C. albicans* and *E. faecalis* are as distantly related as mammals and bacteria, we show that the two microbes — together — complete a metabolic cycle that be both mutually beneficial and antagonistic.

References

Antranikian, G., & Giffhorn, F. (1987). Citrate metabolism in anaerobic bacteria. *FEMS Microbiology Letters*, *46*(2), 175–198. https://doi.org/10.1111/j.1574-6968.1987.tb02458.x

Archambaud, C., Derré-Bobillot, A., Lapaque, N., Rigottier-Gois, L., & Serror, P. (2019). Intestinal translocation of enterococci requires a threshold level of enterococcal overgrowth in the lumen. *Scientific Reports*, *9*(1), 8926. https://doi.org/10.1038/s41598-019-45441-3

Carsanba, E., Papanikolaou, S., Fickers, P., Agirman, B., & Erten, H. (2019). Citric Acid Production by Yarrowia lipolytica. In A. Sibirny (Ed.), *Non-conventional Yeasts: from Basic Research to Application* (pp. 91–117). https://doi.org/10.1007/978-3-030-21110-3

Daca, A., & Jarzembowski, T. (2024). From the Friend to the Foe—Enterococcus faecalis Diverse Impact on the Human Immune System. *International Journal of Molecular Sciences*, *25*(4), 2422. https://doi.org/10.3390/ijms25042422

Du, C., Li, Y., Xiang, R., & Yuan, W. (2022). Formate Dehydrogenase Improves the Resistance to Formic Acid and Acetic Acid Simultaneously in Saccharomyces cerevisiae. *International Journal of Molecular Sciences*, *23*(6), 3406. https://doi.org/10.3390/ijms23063406

Fourie, R., Kuloyo, O. O., Mochochoko, B. M., Albertyn, J., & Pohl, C. H. (2018). Iron at the Centre of Candida albicans Interactions. *Frontiers in Cellular and Infection Microbiology*, *8*, 185. https://doi.org/10.3389/fcimb.2018.00185

Garcia-Santamarina, S., Kuhn, M., Devendran, S., Maier, L., Driessen, M., Mateus, A., Mastrorilli, E., Brochado, A. R., Savitski, M. M., Patil, K. R., Zimmermann, M., Bork, P., & Typas, A. (2024). Emergence of community behaviors in the gut microbiota upon drug treatment. *Cell*. https://doi.org/10.1016/j.cell.2024.08.037

Gould, A. L., Zhang, V., Lamberti, L., Jones, E. W., Obadia, B., Korasidis, N., Gavryushkin, A., Carlson, J. M., Beerenwinkel, N., & Ludington, W. B. (2018). Microbiome interactions shape host fitness. *Proceedings of the National Academy of Sciences*, *115*(51), E11951–E11960. https://doi.org/10.1073/pnas.1809349115

Haas, B. J., Chin, M., Nusbaum, C., Birren, B. W., & Livny, J. (2012). How deep is deep enough for RNA-Seq profiling of bacterial transcriptomes? *BMC Genomics*, *13*(1), 734. https://doi.org/10.1186/1471-2164-13-734

Hattab, S., Dagher, A.-M., & Wheeler, R. T. (2022). Pseudomonas Synergizes with Fluconazole against Candida during Treatment of Polymicrobial Infection. *Infection and Immunity*, *90*(4), e00626-21. https://doi.org/10.1128/iai.00626-21

Hugenholtz, J. (1993). Citrate metabolism in lactic acid bacteria. *FEMS Microbiology Reviews*, *12*(1-3), 165–178. https://doi.org/10.1111/j.1574-6976.1993.tb00017.x

Hughes, E. R. (2017). Microbial Respiration and Formate Oxidation as Metabolic Signatures of Inflammation-Associated Dysbiosis. *Cell Host & Microbe*, *21*(2), 208–219. https://doi.org/10.1016/j.chom.2017.01.005

Książek, E. (2023). Citric Acid: Properties, Microbial Production, and Applications in Industries. *Molecules*, *29*(1), 22. https://doi.org/10.3390/molecules29010022

Kumamoto, C. A., Gresnigt, M. S., & Hube, B. (2020). The gut, the bad and the harmless: Candida albicans as a commensal and opportunistic pathogen in the intestine. *Current Opinion in Microbiology*, *56*, 7–15. https://doi.org/10.1016/j.mib.2020.05.006

Mann, E. R., Lam, Y. K., & Uhlig, H. H. (2024). Short-chain fatty acids: linking diet, the microbiome and immunity. *Nature Reviews Immunology*, *24*(8), 577–595. https://doi.org/10.1038/s41577-024-01014-8

Martino, G. P., Perez, C. E., Magni, C., & Blancato, V. S. (2018). Implications of the expression of Enterococcus faecalis citrate fermentation genes during infection. *PLoS ONE*, *13*(10), e0205787. https://doi.org/10.1371/journal.pone.0205787

Mould, D. L., Finger, C. E., Conaway, A., Botelho, N., Stuut, S. E., & Hogan, D. A. (2024). Citrate cross-feeding by Pseudomonas aeruginosa supports lasR mutant fitness. *MBio*, *15*(2), e01278-23. https://doi.org/10.1128/mbio.01278-23

Pietzke, M., Meiser, J., & Vazquez, A. (2020). Formate metabolism in health and disease. *Molecular Metabolism*, *33*, 23–37. https://doi.org/10.1016/j.molmet.2019.05.012

Ramsey, M., Hartke, A., & Huycke, M. (2014). The Physiology and Metabolism of Enterococci. In M. Gilmore, D. B. Clewell, Y. Ike, & N. Shankar (Eds.), *Enterococci From Commensals to Leading Causes of Drug Resistant Infection*.

Reese, A. T., Pereira, F. C., Schintlmeister, A., Berry, D., Wagner, M., Hale, L. P., Wu, A., Jiang, S., Durand, H. K., Zhou, X., Premont, R. T., Diehl, A. M., O'Connell, T. M., Alberts, S. C., Kartzinel, T. R., Pringle, R. M., Dunn, R. R., Wright, J. P., & David, L. A. (2018). Microbial nitrogen limitation in the mammalian large intestine. *Nature Microbiology*, *3*(12), 1441–1450. https://doi.org/10.1038/s41564-018-0267-7

Rosenkrantz, M., Kell, C. S., Pennell, E. A., Webster, M., & Devenish, L. J. (1994). Distinct upstream activation regions for glucose-repressed and derepressed expression of the yeast citrate synthase gene CIT1. *Current Genetics*, *25*(3), 185–195. https://doi.org/10.1007/bf00357161

Wang, K., Liu, Y., Wu, Z., Wu, Y., Bi, H., Liu, Y., Wang, M., Chen, B., Nielsen, J., Liu, Z., & Tan, T. (2023). Investigating formate tolerance mechanisms in Saccharomyces cerevisiae and its application. *Green Carbon*, *1*(1), 65–74. https://doi.org/10.1016/j.greenca.2023.08.003

Zaheer, R., Noyes, N., Polo, R. O., Cook, S. R., Marinier, E., Domselaar, G. V., Belk, K. E., Morley, P. S., & McAllister, T. A. (2018). Impact of sequencing depth on the characterization of the microbiome and resistome. *Scientific Reports*, *8*(1), 5890. https://doi.org/10.1038/s41598-018-24280-8

Zeng, X., Xing, X., Gupta, M., Keber, F. C., Lopez, J. G., Lee, Y.-C. J., Roichman, A., Wang, L., Neinast, M. D., Donia, M. S., Wühr, M., Jang, C., & Rabinowitz, J. D. (2022). Gut bacterial nutrient preferences quantified in vivo. *Cell*, *185*(18), 3441-3456.e19. https://doi.org/10.1016/j.cell.2022.07.020

Zhai, B., Ola, M., Rolling, T., Tosini, N. L., Joshowitz, S., Littmann, E. R., Amoretti, L. A., Fontana, E., Wright, R. J., Miranda, E., Veelken, C. A., Morjaria, S. M., Peled, J. U., Brink, M. R. M. van den, Babady, N. E., Butler, G., Taur, Y., & Hohl, T. M. (2020). High-resolution mycobiota analysis reveals dynamic intestinal translocation preceding invasive candidiasis. *Nature Medicine*, *26*(1), 59–64. https://doi.org/10.1038/s41591-019-0709-7

Publishing Agreement

It is the policy of the University to encourage open access and broad distribution of all theses, dissertations, and manuscripts. The Graduate Division will facilitate the distribution of UCSF theses, dissertations, and manuscripts to the UCSF Library for open access and distribution. UCSF will make such theses, dissertations, and manuscripts accessible to the public and will take reasonable steps to preserve these works in perpetuity.

I hereby grant the non-exclusive, perpetual right to The Regents of the University of California to reproduce, publicly display, distribute, preserve, and publish copies of my thesis, dissertation, or manuscript in any form or media, now existing or later derived, including access online for teaching, research, and public service purposes.

Signed by:
Haley Gause
40B53B4BF0B148D...

Author Signature

12/3/2024

Date